The topological derivative in anisotropic elasticity

Marc Bonnet, Gabriel Delgado

THE TOPOLOGICAL DERIVATIVE IN ANISOTROPIC ELASTICITY

MARC BONNET[A], GABRIEL DELGADO[B,C]

ABSTRACT. A comprehensive treatment of the topological derivative for anisotropic elasticity is presented, with both the background material and the trial small inhomogeneity assumed to have arbitrary anisotropic elastic properties. A formula for the topological derivative of any cost functional defined in terms of regular volume or surface densities depending on the displacement is established, by combining small-inhomogeneity asymptotics and the adjoint solution approach. The latter feature makes the proposed result simple to implement and computationally efficient. Both three-dimensional and plane-strain settings are treated; they differ mostly on details in the elastic moment tensor (EMT). Moreover, the main properties of the EMT, a critical component of the topological derivative, are studied for the fully anisotropic case. Then, the topological derivative of strain energy-based quadratic cost functionals is derived, which requires a distinct treatment. Finally, numerical experiments on the numerical evaluation of the EMT and the topological derivative of the compliance cost functional are reported.

1. Introduction. The concept of topological derivative appeared in [**1**] and [**2**] in the context of topological optimization of mechanical structures. The topological derivative $DJ(\boldsymbol{z})$ quantifies the perturbation induced to a cost functional J by the virtual creation of an object $B_a(\boldsymbol{z})$ (e.g. a cavity or an inhomogeneity) of vanishingly small characteristic radius a at a prescribed location $\boldsymbol{z}$ inside the solid. In structural optimization, computing the field $DJ(\boldsymbol{z})$ directs the algorithm towards optimal topologies by indicating where creating new holes is most profitable from the featured cost functional viewpoint, an approach used by e.g. [**3**], and also [**4**] in conjunction with the shape derivative, while applications to shape optimization problems include [**5**]. Moreover, the topological derivative has been found to be also very useful as a means of defining a defect indicator function in flaw identification problems, see e.g. [**6, 7, 8, 9**]. Such optimization or inverse problems usually feature cost functionals that involve volume or surface integrals of densities that depend on the displacement solving (in the present context) an elastostatic equilibrium problem on the reference solid. Moreover, constitutive or flaw identification problems are sometimes formulated in terms of energy cost functionals (e.g. of the Kohn-Vogelius type [**10**] or error in constitutive equation functionals [**11, 12**]), whose densities depend on displacement gradients.

To establish the expression of the topological sensitivity for a given cost functional and a chosen set of underlying geometrical and physical assumptions, one needs information about the asymptotic behavior as $a \to 0$ of the perturbation induced to the physical field variable (e.g. displacement) by the virtual creation of $B_a(\boldsymbol{z})$. An abundant literature is available on such asymptotic analyses, see e.g. [**13, 14, 15, 16, 17**]. A key component for computationally efficient topological derivative formulations is the adjoint solution method which, like with other types of sensitivity analysis, provides a valuable computational shortcut by replacing the computation of many sensitivity fields (in the present context, one sensitivity field for each virtual nucleation site $\boldsymbol{z}$ used in the computation) by that of just one adjoint solution. Adjoint solutions for topological sensitivity appeared in [**18, 19**] and thence found more widespread use, see e.g. [**20, 21, 7, 9**]. Another important component of topological derivative formulas is the elastic moment tensor (EMT), whose definition and properties are extensively studied in e.g. [**22**] for the isotropic case and [**23, 24**] for the anisotropic case.

Within the present framework of linear elasticity, results available for small-inhomogeneity asymptotic expansions, as well as their application to the concept of topological derivative, often assume isotropic elasticity, see e.g. [**25, 26, 18, 27, 20**]. Comparatively scarce material is available for the topological derivative in the more-general case of anisotropic elasticity. It includes the formulation of the elasto-dynamic topological derivative for arbitrary surface-integral cost functionals [**28, 29**] and that of small-inhomogeneity solution asymptotics for anisotropic materials [**30, 31, 23, 24**]. Moreover, the topological derivative of energy-based cost functionals has also been sparsely addressed so far (notably in [**21**] for Stokes flows).

The main purpose of this paper is to present a comprehensive treatment of the topological derivative for anisotropic elasticity, with the background material and the small trial inhomogeneity both allowed to have anisotropic properties. A formula for the topological derivative of any cost functional defined in terms of regular volume or surface densities depending on the displacement is established, by combining small-inhomogeneity asymptotics and the adjoint solution approach. The latter feature makes the proposed result simple to implement and computationally efficient. Both three-dimensional and plane-strain settings are covered; they differ mostly on details pertaining to the EMT. This result directly generalizes previously-known formulations for isotropic elasticity to the fully anisotropic case. Moreover, the topological derivative of strain energy-based cost functionals, which depend on the displacement gradient, is also established. This case, seldom addressed so far, requires a specific, and separate, treatment, due to the fact that the *strain* perturbation in B_a does not vanish in the limit $a \to 0$ (whereas the displacement itself does vanish). The practical computation of the EMT for general anisotropy, which is necessary in practical applications of the topological derivative, is also addressed. Actual or potential applications of the results presented in this article include topology optimization of composite structures, a topic currently pursued by the second author of this article, or flaw identification using experimental data from nondestructive testing. Both types of problems may be cast as minimization problems, in which case the spatial locations where negative values of the topological derivative occur are selected for material modification or as the likeliest locations of flaws to be detected, depending on the objective.

This article is organised as follows. Section 2 introduces notation and collects background material on the elastic transmission problem, elastic moment tenors, cost functionals and the concept of topological derivative. The small-inhomogeneity asymptotics for the solution and the featured class of cost functionals are obtained in Secs. 3 and 4, respectively. Then, the specific treatment needed for deriving the small-inhomogeneity asymptotics of energy-based cost functionals is presented in Sec. 5. Finally, numerical experiments on the topological derivative of the compliance cost functional, the numerical evaluation of the EMT and a flaw identification problem are presented in Sec. 6.

2. Elastic transmission problem, cost functional and topological derivative.

2.1. Notation, elastic transmission problem. Consider an elastic body occupying a smooth bounded domain $\Omega \subset \mathbb{R}^3$. The anisotropic elastic properties of the background material (against which the effect of small inhomogeneities will be considered), assumed to be homogeneous, are characterized by the fourth-order elasticity tensor $\boldsymbol{\mathcal{C}}$. The boundary $\partial\Omega$ is split according to $\partial\Omega = \Gamma_{\mathrm{D}} \cup \Gamma_{\mathrm{N}}$ (where $\Gamma_{\mathrm{D}} \cap \Gamma_{\mathrm{N}} = \emptyset$ and $|\Gamma_{\mathrm{D}}| \neq 0$), so that a given force density $\boldsymbol{g} \in L^2(\Gamma_{\mathrm{N}};\mathbb{R}^3)$ is applied on Γ_{N} while a given displacement $\bar{\boldsymbol{u}} \in H^{1/2}(\Gamma_{\mathrm{D}};\mathbb{R}^3)$ is prescribed on Γ_{D}. Additionally, a body force density $\boldsymbol{f} \in L^2(\Omega;\mathbb{R}^3)$ is applied to Ω.

The background solution, i.e. the displacement field arising in the reference solid due to the prescribed excitations $(\boldsymbol{f}, \boldsymbol{g}, \bar{\boldsymbol{u}})$, is defined as the solution to

$$\mathrm{div}(\boldsymbol{\mathcal{C}}\!:\!\boldsymbol{\varepsilon}[\boldsymbol{u}]) + \boldsymbol{f} = \boldsymbol{0} \text{ in } \Omega, \quad \boldsymbol{t}[\boldsymbol{u}] = \boldsymbol{g} \text{ on } \Gamma_{\mathrm{N}}, \quad \boldsymbol{u} = \bar{\boldsymbol{u}} \text{ on } \Gamma_{\mathrm{D}} \tag{1}$$

where $\boldsymbol{\varepsilon}[\boldsymbol{w}]$ and $\boldsymbol{t}[\boldsymbol{w}]$ denote the linearized strain tensor and the traction vector associated with a given displacement $\boldsymbol{w}$, respectively defined by

$$\text{(a)} \quad \boldsymbol{\varepsilon}[\boldsymbol{u}] = \tfrac{1}{2}(\boldsymbol{\nabla u} + \boldsymbol{\nabla u}^{\mathrm{T}}), \qquad \text{(b)} \quad \boldsymbol{t}[\boldsymbol{u}] = (\boldsymbol{\mathcal{C}}\!:\!\boldsymbol{\varepsilon}[\boldsymbol{u}])\cdot\boldsymbol{n} \tag{2}$$

(with $\boldsymbol{n}$ the unit outward normal to Ω). In (2b) and hereinafter, symbols '$\cdot$' and '$:$' denote single and double inner products, e.g. $(\boldsymbol{E}\cdot\boldsymbol{x})_i = E_{ij}x_j$ and $(\boldsymbol{\mathcal{C}} : \boldsymbol{E})_{ij} = \mathcal{C}_{ijk\ell}E_{k\ell}$, with Einstein's convention of summation over repeated indices implicitly used throughout.

Alternatively, the background displacement is governed by the weak formulation

$$\text{Find } \boldsymbol{u} \in W(\bar{\boldsymbol{u}}), \qquad \langle \boldsymbol{u}, \boldsymbol{w}\rangle_{\Omega}^{\mathcal{C}} = F(\boldsymbol{w}), \quad \forall \boldsymbol{w} \in W_0, \tag{3}$$

where $\langle \boldsymbol{u}, \boldsymbol{w}\rangle_{D}^{\mathcal{C}}$ denotes the bilinear elastic energy form associated to given domain $D \subset \mathbb{R}^3$ and elasticity tensor $\boldsymbol{\mathcal{C}}$, i.e.:

$$\langle \boldsymbol{u}, \boldsymbol{w}\rangle_{D}^{\mathcal{C}} := \int_D \boldsymbol{\varepsilon}[\boldsymbol{u}]\!:\!\boldsymbol{\mathcal{C}}\!:\!\boldsymbol{\varepsilon}[\boldsymbol{w}]\,\mathrm{d}V = \int_D \boldsymbol{\nabla u}\!:\!\boldsymbol{\mathcal{C}}\!:\!\boldsymbol{\nabla w}\,\mathrm{d}V \tag{4}$$

(with the second equality holding by virtue of the well-known major symmetry of $\boldsymbol{\mathcal{C}}$), the linear form F associated to the loading is defined by

$$F(\boldsymbol{w}) = \int_\Omega \boldsymbol{f}\cdot\boldsymbol{w}\,\mathrm{d}V + \int_{\Gamma_\mathrm{N}} \boldsymbol{g}\cdot\boldsymbol{w}\,\mathrm{d}S, \tag{5}$$

and having introduced, for given $\bar{\boldsymbol{u}} \in H^{1/2}(\Gamma_\mathrm{D};\mathbb{R}^3)$, the spaces $W(\bar{\boldsymbol{u}})$ and W_0 of displacement fields that are kinematically admissible with respect to arbitrary and homogeneous prescribed Dirichlet data, respectively, i.e.:

$$W(\bar{\boldsymbol{u}}) := \big\{\boldsymbol{v}\in H^1(\Omega;\mathbb{R}^3),\, \boldsymbol{v}=\bar{\boldsymbol{u}} \text{ on } \Gamma_\mathrm{D}\big\}, \qquad W_0 := W(\boldsymbol{0}). \tag{6}$$

The assumption $\boldsymbol{f}\in L^2(\Omega;\mathbb{R}^3)$ implies that the solution $\boldsymbol{u}$ of problem (3) has in fact $H^2_{\mathrm{loc}}(\Omega;\mathbb{R}^3)$ interior regularity (see e.g. **[32]**, Thm. 6.3-6 and p. 298), and hence that $\boldsymbol{u}\in C^0(D)$ for any subset $D \Subset \Omega$ by the Sobolev embedding theorem.

Well-known properties of elasticity tensors are now recalled for convenience. For general anisotropic materials, the elasticity tensor $\boldsymbol{\mathcal{C}}$ is positive definite (in the sense that $\boldsymbol{E}:\boldsymbol{\mathcal{C}}:\boldsymbol{E} > 0$ for any symmetric second-order tensor $\boldsymbol{E}\in\mathbb{R}^{3,3}_{\mathrm{sym}}$, $\boldsymbol{E}\neq\boldsymbol{0}$ and has the major and minor symmetries (i.e. $\mathcal{C}_{ijk\ell}=\mathcal{C}_{k\ell ij}=\mathcal{C}_{jik\ell}=\mathcal{C}_{ij\ell k}$); it may thus involve up to 21 independent elastic constants. For isotropic materials characterized by their bulk modulus κ and shear modulus μ, $\boldsymbol{\mathcal{C}}$ is given by

$$\boldsymbol{\mathcal{C}} = 3\kappa\boldsymbol{\mathcal{J}} + 2\mu\boldsymbol{\mathcal{K}}, \tag{7}$$

where $\boldsymbol{\mathcal{J}},\boldsymbol{\mathcal{K}}$ are fourth-order tensors respectively defined by $\boldsymbol{\mathcal{J}} = (1/3)\boldsymbol{I}\otimes\boldsymbol{I}$ and $\boldsymbol{\mathcal{K}} = \boldsymbol{\mathcal{I}} - \boldsymbol{\mathcal{J}}$ (with $\boldsymbol{I}$ and $\boldsymbol{\mathcal{I}}$ denoting the second-order identity and the fourth-order identity for symmetric tensors, respectively), so that $\boldsymbol{E} = \boldsymbol{\mathcal{J}}:\boldsymbol{E} + \boldsymbol{\mathcal{K}}:\boldsymbol{E}$ is the decomposition of a symmetric second-order tensor $\boldsymbol{E}\in\mathbb{R}^{3,3}_{\mathrm{sym}}$ into its spherical and deviatoric parts.

2.2. Transmission problem for a small trial inhomogeneity. Now, consider a single small elastic inhomogeneity located at $\boldsymbol{z}\in\Omega$, of characteristic linear size a, occupying the domain

$$B_a = \boldsymbol{z} + a\mathcal{B},$$

where $\mathcal{B}$ is a bounded smooth domain of $\mathbb{R}^3$ and a is small enough so that $\bar{B}_a \Subset \Omega$. The inhomogeneity is endowed with anisotropic elastic properties characterized by the elasticity tensor $\boldsymbol{\mathcal{C}}^\star$, so that the elastic properties of the whole solid are defined by the tensor-valued field $\boldsymbol{\mathcal{C}}_a$ such that

$$\boldsymbol{\mathcal{C}}_a = (1-\chi(B_a))\boldsymbol{\mathcal{C}} + \chi(B_a)\boldsymbol{\mathcal{C}}^\star = \boldsymbol{\mathcal{C}} + \chi(B_a)\Delta\boldsymbol{\mathcal{C}}, \tag{8}$$

$\chi(D)$ being the characteristic function of the domain D and $\Delta\boldsymbol{\mathcal{C}} := \boldsymbol{\mathcal{C}}^\star - \boldsymbol{\mathcal{C}}$ denoting the elastic tensor perturbation.

The displacement field $\boldsymbol{u}_a\in W(\bar{\boldsymbol{u}})$ arising in the solid containing the small inhomogeneity due to the prescribed excitations $(\boldsymbol{f},\boldsymbol{g},\bar{\boldsymbol{u}})$ solves the transmission problem

$$\mathrm{div}(\boldsymbol{\mathcal{C}}_a:\boldsymbol{\varepsilon}[\boldsymbol{u}_a]) + \boldsymbol{f} = \boldsymbol{0} \text{ in } \Omega, \quad \boldsymbol{t}[\boldsymbol{u}_a] = \boldsymbol{g} \text{ on } \Gamma_\mathrm{N}, \quad \boldsymbol{u} = \bar{\boldsymbol{u}}_a \text{ on } \Gamma_\mathrm{D} \tag{9}$$

or, equivalently, the weak formulation

$$\text{Find } \boldsymbol{u}_a\in W(\bar{\boldsymbol{u}}), \qquad \langle\boldsymbol{u}_a,\boldsymbol{w}\rangle_\Omega^{\mathcal{C}_a} = F(\boldsymbol{w}), \quad \forall\boldsymbol{w}\in W_0. \tag{10}$$

Either formulation (9) or (10) implicitly enforces the perfect-bonding relations $\boldsymbol{u}_a|_+ = \boldsymbol{u}_a|_-$ and $\boldsymbol{t}[\boldsymbol{u}_a]|_+ = \boldsymbol{t}^\star[\boldsymbol{u}_a]|_-$ on ∂B_a, where the $\pm$ subscripts indicate limiting values from outside and inside B_a, respectively, and with the traction operator $\boldsymbol{w}\mapsto\boldsymbol{t}^\star[\boldsymbol{w}]$ defined by (2b) with $\boldsymbol{\mathcal{C}}$ replaced with $\boldsymbol{\mathcal{C}}^\star$ (both $\boldsymbol{t}[\cdot]$ and $\boldsymbol{t}^\star[\cdot]$ being conventionally associated with the unit outward normal vector to B_a). The solution $\boldsymbol{u}_a$ of (10) *a priori* belongs to $H^2_{\mathrm{loc}}\big((\Omega\setminus\bar{B}_a)\cup B_a\,;\mathbb{R}^3\big)$, and therefore to $C^0(D)$ for any subset $D \Subset \big((\Omega\setminus\bar{B}_a)\cup B_a\big)$. To later permit Taylor expansions of displacements or strains about $\boldsymbol{z}$, the body force density $\boldsymbol{f}$ is in fact assumed to have local $C^{0,\beta}(V)$ regularity for some $\beta>0$ in a neighbourhood V of $\boldsymbol{z}$, ensuring (e.g. from the properties of elastic volume potentials, see **[33]**, Thm. 10.4) that $\boldsymbol{u}$ is in $C^{2,\beta}(D)$ for any subset $D \Subset V$.

One notes for later reference that the potential energy $E_{\rm pot}$ of the solution $\boldsymbol{u}_a$ to (10) is given by

$$E_{\rm pot}(\boldsymbol{\mathcal{C}}_a) = \mathbb{E}_{\rm pot}(\boldsymbol{u}_a) = \tfrac{1}{2}\langle \boldsymbol{u}_a, \boldsymbol{u}_a\rangle_\Omega^{\mathcal{C}_a} - F(\boldsymbol{u}_a) = -\tfrac{1}{2}F(\boldsymbol{u}_a) \tag{11}$$

where the second equality exploits (10) and holds provided that $\boldsymbol{u}_a \in W_0$, i.e. only for problems with homogeneous Dirichlet data $\bar{\boldsymbol{u}} = \boldsymbol{0}$ on $\Gamma_{\rm D}$.

It will be convenient for our purposes to exploit a formulation of the transmision problem (10) in terms of the displacement perturbation $\boldsymbol{v}_a := \boldsymbol{u}_a - \boldsymbol{u}$ rather than the total displacement $\boldsymbol{u}_a$. The following governing weak formulation for $\boldsymbol{v}_a$ is easily obtained by subtracting (3) from (10):

$$\text{Find } \boldsymbol{v}_a \in W_0, \quad \langle \boldsymbol{v}_a, \boldsymbol{w}\rangle_\Omega^{\mathcal{C}_a} = -\langle \boldsymbol{u}, \boldsymbol{w}\rangle_{B_a}^{\Delta\mathcal{C}}, \quad \forall \boldsymbol{w} \in W_0. \tag{12}$$

Free-space transmission problem (FSTP).. The auxiliary problem of a perfectly-bonded inhomogeneity $(\mathcal{B}, \boldsymbol{\mathcal{C}}^\star)$ embedded in an infinite elastic medium $\Omega = \mathbb{R}^3$ subjected to a uniform remote stress will play an important role in the sequel and is thus given now for later reference together with some additional useful notation. For an arbitrary constant second-order tensor $\boldsymbol{E} \in \mathbb{R}^{3,3}$, let $\boldsymbol{\varphi}[\boldsymbol{E}]$ denote the linear vector-valued function defined by

$$\boldsymbol{\varphi}[\boldsymbol{E}](\boldsymbol{\xi}) := \boldsymbol{E}\cdot\boldsymbol{\xi}. \tag{13}$$

Let the background solution $\boldsymbol{u}$ be chosen as $\boldsymbol{u} = \boldsymbol{\varphi}[\boldsymbol{E}]$, noting that $\mathrm{div}(\boldsymbol{\mathcal{C}} : \boldsymbol{\nabla}\boldsymbol{\varphi}[\boldsymbol{E}]) = \boldsymbol{0}$. The FSTP consists in finding the displacement field $\boldsymbol{u}_{\mathcal{B}}[\boldsymbol{E}]$ such that

$$\mathrm{div}(\boldsymbol{\mathcal{C}}_{\mathcal{B}} : \boldsymbol{\nabla}\boldsymbol{u}_{\mathcal{B}}[\boldsymbol{E}]) = \boldsymbol{0} \ \text{ in } \mathbb{R}^3, \qquad \boldsymbol{u}_{\mathcal{B}}[\boldsymbol{E}](\boldsymbol{\xi}) - \boldsymbol{\varphi}[\boldsymbol{E}](\boldsymbol{\xi}) = O(|\boldsymbol{\xi}|^{-2}) \ \ (|\boldsymbol{\xi}| \to \infty) \tag{14}$$

where

$$\boldsymbol{\mathcal{C}}_{\mathcal{B}} = (1 - \chi(\mathcal{B}))\boldsymbol{\mathcal{C}} + \chi(\mathcal{B})\boldsymbol{\mathcal{C}}^\star = \boldsymbol{\mathcal{C}} + \chi(\mathcal{B})\Delta\boldsymbol{\mathcal{C}}$$

The FSTP (14) is analytically solved for an ellipsoidal inhomogeneity in Eshelby's landmark paper **[34]**. It can be recast into the following weak formulation for the displacement perturbation $\boldsymbol{v}_{\mathcal{B}}[\boldsymbol{E}] := \boldsymbol{u}_{\mathcal{B}}[\boldsymbol{E}] - \boldsymbol{\varphi}[\boldsymbol{E}]$:

$$\text{Find } \boldsymbol{v}_{\mathcal{B}}[\boldsymbol{E}] \in W_\infty, \langle \boldsymbol{v}_{\mathcal{B}}[\boldsymbol{E}], \boldsymbol{w}\rangle_{\mathbb{R}^3}^{\mathcal{C}_{\mathcal{B}}} = -\langle \boldsymbol{\varphi}[\boldsymbol{E}], \boldsymbol{w}\rangle_{\mathcal{B}}^{\Delta\mathcal{C}}, \quad \forall \boldsymbol{w} \in W_\infty, \tag{15}$$

with the function space W_∞ defined by $W_\infty = \left\{ \boldsymbol{w} \in L^2_{\rm loc}(\mathbb{R}^3;\mathbb{R}^3), \boldsymbol{\nabla}\boldsymbol{w} \in L^2(\mathbb{R}^3;\mathbb{R}^{3,3}) \right\}$. Note that $\langle \boldsymbol{\varphi}[\boldsymbol{E}], \boldsymbol{w}\rangle_{\mathcal{B}}^{\Delta\mathcal{C}} = \langle \boldsymbol{\varphi}[\boldsymbol{E}^{\rm T}], \boldsymbol{w}\rangle_{\mathcal{B}}^{\Delta\mathcal{C}}$, implying that $\boldsymbol{v}_{\mathcal{B}}[\boldsymbol{E}]$ solving (15) depends only on the symmetric part $\boldsymbol{E}_{\rm sym} := \frac{1}{2}(\boldsymbol{E} + \boldsymbol{E}^{\rm T}) \in \mathbb{R}^{3,3}_{\rm sym}$ of $\boldsymbol{E}$.

2.3. Cost functional and topological derivative. Now, cost functionals $J(\boldsymbol{\mathcal{C}}_a)$ of the form

$$J(\boldsymbol{\mathcal{C}}_a) = \mathbb{J}(\boldsymbol{u}_a) \quad \text{with} \ \ \mathbb{J}(\boldsymbol{w}) := \int_\Omega \psi_\Omega(\boldsymbol{x}, \boldsymbol{w}) \, \mathrm{d}V(\boldsymbol{x}) + \int_{\partial\Omega} \psi_\Gamma(\boldsymbol{x}, \boldsymbol{w}) \, \mathrm{d}S(\boldsymbol{x}) \tag{16}$$

are considered, where the density functions $\psi_\Omega, \psi_\Gamma : (\mathbb{R}^3 \times \mathbb{R}^3) \to \mathbb{R}$ are twice differentiable with respect to their second argument and are assumed to obey the growth conditions

$$\begin{aligned} &|\psi_\Omega(\boldsymbol{x}, \boldsymbol{w})| \le C(1 + |\boldsymbol{w}|^2), \qquad |\psi'_\Omega(\boldsymbol{x}, \boldsymbol{w})| \le C(1 + |\boldsymbol{w}|) \qquad |\psi''_\Omega(\boldsymbol{x}, \boldsymbol{w})| \le C \\ &|\psi_\Gamma(\boldsymbol{x}, \boldsymbol{w})| \le C(1 + |\boldsymbol{w}|^2), \qquad |\psi'_\Gamma(\boldsymbol{x}, \boldsymbol{w})| \le C(1 + |\boldsymbol{w}|) \qquad |\psi''_\Gamma(\boldsymbol{x}, \boldsymbol{w})| \le C \end{aligned} \tag{17}$$

(with ψ' and ψ'' denoting the gradient and Hessian, respectively, of ψ with respect to its second argument and C being some positive constant), so as to ensure that $\mathbb{J}$ and its first and second-order directional derivatives are defined for any $\boldsymbol{w} \in H^1(\Omega;\mathbb{R}^3)$. Typical examples of cost functionals include the elastic potential energy $\mathbb{E}_{\rm pot}$, with

$$\psi_\Omega(\boldsymbol{\xi}, \boldsymbol{w}) = -\tfrac{1}{2}\boldsymbol{w}\cdot\boldsymbol{f}(\boldsymbol{\xi}), \qquad \psi_\Gamma(\boldsymbol{\xi}, \boldsymbol{w}) = -\tfrac{1}{2}\boldsymbol{w}\cdot\boldsymbol{g}(\boldsymbol{\xi}),$$

(if $\bar{\boldsymbol{u}} = \boldsymbol{0}$, and using (11) in that case) and weighted least-squares misfit functionals used for e.g. flaw identification problems, with

$$\psi_\Omega(\boldsymbol{\xi}, \boldsymbol{w}) = 0, \qquad \psi_\Gamma(\boldsymbol{\xi}, \boldsymbol{w}) = \tfrac{1}{2}\chi(S_{\rm obs})(\boldsymbol{w} - \boldsymbol{u}_{\rm obs}(\boldsymbol{\xi}))^{\rm T}\cdot\boldsymbol{W}(\boldsymbol{\xi})\cdot(\boldsymbol{w} - \boldsymbol{u}_{\rm obs}(\boldsymbol{\xi})).$$

and where $\boldsymbol{\xi} \mapsto \boldsymbol{W}(\boldsymbol{\xi})$ is a positive-definite matrix-valued function, $S_{\rm obs} \subset \Gamma_{\rm N}$ is the measurement surface and $\boldsymbol{u}_{\rm obs}$ the measured value of $\boldsymbol{u}$ on $S_{\rm obs}$.

Definition 1 (topological derivative)**.** *Assume that $J(\mathcal{C}_a)$ can be expanded in the form*

$$J(\mathcal{C}_a) = J(\mathcal{C}) + \delta(a) DJ(\boldsymbol{z}) + o(\delta(a)) \tag{18}$$

where $\delta(a)$ is assumed to vanish as $a \to 0$ and characterizes the small-inhomogeneity asymptotic behavior of $J(\mathcal{C}_a)$. Then, the coefficient $DJ(\boldsymbol{z})$, which also depends a priori on the shape $\mathcal{B}$ and the moduli $\mathcal{C}, \mathcal{C}^\star$, is called the topological derivative *of J at $\boldsymbol{z} \in \Omega$.*

Remark 1. *Terminology for the concept of topological derivative varies, with "gradient" or "sensitivity" used instead of "derivative" in some publications.*

2.4. Elastic moment tensor. The elastic moment tensor, which will be seen to play a central role in the small-inhomogeneity asymptotics of $J(\mathcal{C}_a)$, is now defined.

Definition 2 (elastic moment tensor)**.** *Let $\boldsymbol{v}_{\mathcal{B}}[\boldsymbol{E}]$ denote the solution to the FSTP* (15) *for given $\boldsymbol{E} \in \mathbb{R}^{3,3}$. The (fourth-order)* elastic moment tensor *(EMT) $\boldsymbol{\mathcal{A}}$ is defined by*

$$\boldsymbol{\mathcal{A}} : \boldsymbol{E} = \int_{\mathcal{B}} \Delta\mathcal{C} : \boldsymbol{\nabla} \boldsymbol{u}_{\mathcal{B}}[\boldsymbol{E}] \; dV = \int_{\mathcal{B}} \Delta\mathcal{C} : (\boldsymbol{E} + \boldsymbol{\nabla} \boldsymbol{v}_{\mathcal{B}}[\boldsymbol{E}]) \; dV \qquad \forall \boldsymbol{E} \in \mathbb{R}^{3,3}. \tag{19}$$

Remark 2. *In* **[22, 17]***, the EMT is defined, for isotropic materials, in terms of the densities of two elastic layer potentials that are used there to formulate the FSTP* (14)*. That definition in fact coincides with the present definition* (19)*. To see this, integrating* (19) *by parts, one finds*

$$\boldsymbol{E}' \; : \; \boldsymbol{\mathcal{A}} \; : \; \boldsymbol{E} \;=\; \int_{\partial\mathcal{B}} \big[\boldsymbol{E}' \; : \; (\boldsymbol{\mathcal{C}}^\star \,-\, \boldsymbol{\mathcal{C}}) \cdot \boldsymbol{n}\big] \cdot \boldsymbol{u}_{\mathcal{B}}[\boldsymbol{E}] \; dS \;=\; \int_{\partial\mathcal{B}} \big(\boldsymbol{t}^\star\big[\boldsymbol{\varphi}[\boldsymbol{E}']\big] \,-\, \boldsymbol{t}\big[\boldsymbol{\varphi}[\boldsymbol{E}']\big]\big) \cdot \boldsymbol{u}_{\mathcal{B}}[\boldsymbol{E}] \; dS.$$

This identity coincides (upon adaptation to the present notations) with the left and right contraction of eq. (10.12) in Lemma 10.3 of **[17]** *by two tensors $\boldsymbol{E}, \boldsymbol{E}' \in \mathbb{R}^{3,3}$.*

Properties of the elastic moment tensor. The main known properties of the EMT are now collected.

Proposition 1 (symmetry)**.** *The elastic moment tensor $\boldsymbol{\mathcal{A}}$ has major and minor symmetries: for any pair of second-order tensors $\boldsymbol{E}, \boldsymbol{E}' \in \mathbb{R}^{3,3}$, one has the major symmetry*

$$\boldsymbol{E}' : \boldsymbol{\mathcal{A}} : \boldsymbol{E} = \boldsymbol{E} : \boldsymbol{\mathcal{A}} : \boldsymbol{E}' \tag{20}$$

and the minor symmetries

$$\textit{(i)}\ \boldsymbol{E}' : \boldsymbol{\mathcal{A}} : \boldsymbol{E} = \boldsymbol{E}' : \boldsymbol{\mathcal{A}} : \boldsymbol{E}^T, \quad \textit{(ii)}\ \boldsymbol{E}' : \boldsymbol{\mathcal{A}} : \boldsymbol{E} = \boldsymbol{E}'^T : \boldsymbol{\mathcal{A}} : \boldsymbol{E}. \tag{21}$$

Proof. First, taking the left inner product of Eq. (19) by $\boldsymbol{E}'$, one obtains

$$\boldsymbol{E}' : \boldsymbol{\mathcal{A}} : \boldsymbol{E} = \boldsymbol{E}' : \Big\{ \int_{\mathcal{B}} \Delta\mathcal{C} : \boldsymbol{\nabla} \boldsymbol{v}_{\mathcal{B}}[\boldsymbol{E}] \; \mathrm{d}V \Big\} + \boldsymbol{E}' : \Big\{ \int_{\mathcal{B}} \Delta\mathcal{C} \; \mathrm{d}V \Big\} : \boldsymbol{E} \tag{22}$$

The second term of the above right-hand side is clearly symmetric in $\boldsymbol{E}, \boldsymbol{E}'$ due to the major symmetry of $\Delta\mathcal{C} = \mathcal{C}^\star - \mathcal{C}$, so the symmetry of the first term remains to be proved. To this aim, one starts by noting that, by virtue of definition (4) of $\langle \cdot, \cdot \rangle_{\mathcal{B}}^{\Delta\mathcal{C}}$, one has

$$\boldsymbol{E}' : \Big\{ \int_{\mathcal{B}} \Delta\mathcal{C} : \boldsymbol{\nabla} \boldsymbol{v}_{\mathcal{B}}[\boldsymbol{E}] \; \mathrm{d}V \Big\} = \langle \boldsymbol{\varphi}[\boldsymbol{E}'], \boldsymbol{v}_{\mathcal{B}}[\boldsymbol{E}] \rangle_{\mathcal{B}}^{\Delta\mathcal{C}}. \tag{23}$$

Then, using variational formulation (15) for $\boldsymbol{v}_{\mathcal{B}}[\boldsymbol{E}]$ with $\boldsymbol{w} = = \boldsymbol{v}_{\mathcal{B}}[\boldsymbol{E}']$, one has

$$\begin{aligned} -\langle \boldsymbol{\varphi}[\boldsymbol{E}'], \boldsymbol{v}_{\mathcal{B}}[\boldsymbol{E}] \rangle_{\mathcal{B}}^{\Delta\mathcal{C}} &= \langle \boldsymbol{v}_{\mathcal{B}}[\boldsymbol{E}'], \boldsymbol{v}_{\mathcal{B}}[\boldsymbol{E}] \rangle_{\mathbb{R}^3}^{\mathcal{C}_{\mathcal{B}}} \\ &= \langle \boldsymbol{v}_{\mathcal{B}}[\boldsymbol{E}], \boldsymbol{v}_{\mathcal{B}}[\boldsymbol{E}'] \rangle_{\mathbb{R}^3}^{\mathcal{C}_{\mathcal{B}}} = -\langle \boldsymbol{\varphi}[\boldsymbol{E}], \boldsymbol{v}_{\mathcal{B}}[\boldsymbol{E}'] \rangle_{\mathcal{B}}^{\Delta\mathcal{C}} \end{aligned}$$

(using the symmetry of $\langle \cdot, \cdot \rangle_{\mathbb{R}^3}^{\mathcal{C}_{\mathcal{B}}}$) which, combined with (23) written for $\boldsymbol{E}, \boldsymbol{E}'$ and $\boldsymbol{E}', \boldsymbol{E}$, yields the desired remaining symmetry

$$\boldsymbol{E}' : \Big\{ \int_{\mathcal{B}} \Delta\mathcal{C} : \boldsymbol{\nabla} \boldsymbol{v}_{\mathcal{B}}[\boldsymbol{E}] \, \mathrm{d}V \Big\} = \boldsymbol{E} : \Big\{ \int_{\mathcal{B}} \Delta\mathcal{C} : \boldsymbol{\nabla} \boldsymbol{v}_{\mathcal{B}}[\boldsymbol{E}'] \, \mathrm{d}V \Big\} \tag{24}$$

The major symmetry (20) follows from (22), (24) and the known major symmetry of $\Delta\mathcal{C}$.

Moreover, the minor symmetry (21i) follows immediately from the corresponding minor symmetry of $\Delta\mathcal{C}$. Finally, (20) and (21i) imply (21ii). □

Proposition 2 (scaling)**.** *Let $\mathcal{B}_0$ have the same shape as $\mathcal{B}$ and unit volume (i.e. $\mathcal{B}_0 = |\mathcal{B}|^{-1/3}\mathcal{B}$), and assume that the contrast $\Delta\mathcal{C}$ is uniform. Then, one has*

$$\mathcal{A}(\mathcal{B}, \mathcal{C}, \mathcal{C}^\star) = |\mathcal{B}| \mathcal{A}(\mathcal{B}_0, \mathcal{C}, \mathcal{C}^\star) \tag{25}$$

Proof. Denote by $\boldsymbol{v}_{\mathcal{B}_0}$ the solution to problem (14) for the inhomogeneity $\mathcal{B}_0$, and let $\lambda = |\mathcal{B}|^{1/3}$ be the linear scaling parameter such that $\mathcal{B} = \lambda\mathcal{B}_0$. Then, on setting $(\bar{\boldsymbol{\xi}}, \bar{\boldsymbol{x}}) = \lambda(\bar{\boldsymbol{\xi}}_0, \bar{\boldsymbol{x}}_0)$ in (35), invoking the homogeneity of $\boldsymbol{\nabla}\boldsymbol{G}_\infty$ and essentially repeating arguments already used in the asymptotic analysis of Sec. 3.3, one easily finds that $\boldsymbol{v}_{\mathcal{B}}(\bar{\boldsymbol{\xi}}) = \lambda \boldsymbol{v}_{\mathcal{B}_0}(\bar{\boldsymbol{\xi}}_0)$, and hence $\boldsymbol{\nabla}\boldsymbol{v}_{\mathcal{B}}(\bar{\boldsymbol{\xi}}) = \boldsymbol{\nabla}\boldsymbol{v}_{\mathcal{B}_0}(\bar{\boldsymbol{\xi}}_0)$. Exploiting this remark, and setting $\bar{\boldsymbol{\xi}} = \lambda\bar{\boldsymbol{\xi}}_0$, in (19) then yields the desired result (25). □

The next important property of $\boldsymbol{\mathcal{A}}$ to consider is its sign-definiteness. It can conveniently be formulated in terms of the generalized eigenvalue problem

$$(\mathcal{C}^\star - \Lambda\mathcal{C}) : \boldsymbol{E} = \boldsymbol{0} \qquad (\boldsymbol{E} \in \mathbb{R}^{3,3}_{\mathrm{sym}}), \tag{26}$$

which admits six real and strictly positive eigenvalues $\Lambda_1, \ldots, \Lambda_6$ and associated eigentensors $\boldsymbol{E}_1, \ldots \boldsymbol{E}_6 \in \mathbb{R}^{3,3}_{\mathrm{sym}}$, by virtue of $\mathcal{C}^\star$ and $\mathcal{C}$ defining positive-definite quadratic forms over the six-dimensional vector space $\mathbb{R}^{3,3}_{\mathrm{sym}}$ (i.e. (26) could be recast as a generalized eigenvalue problem for two symmetric positive definite 6×6 matrices, see **[35]**). Moreover, the $\boldsymbol{E}_I$ are $\mathcal{C}$-orthogonal, and can be chosen as $\mathcal{C}$-orthonormal.

Proposition 3 (sign-definiteness)**.** *The elastic moment tensor $\boldsymbol{\mathcal{A}}$ is positive definite if $\Lambda_I > 1$ $(1 \le I \le 6)$, and negative definite if $\Lambda_I < 1$ $(1 \le I \le 6)$. Moreover, if $\Lambda_I = 1$ for some I, then $\boldsymbol{\mathcal{A}} : \boldsymbol{E}_I = \boldsymbol{0}$, i.e. $\boldsymbol{E}_I$ is in the null space of $\boldsymbol{\mathcal{A}}$.*

Remark 3 (isotropic materials)**.** *If both matrix and inhomogeneity materials are isotropic, $\mathcal{C}$ and $\mathcal{C}^\star$ are of the form* (7) *with respective moduli pairs κ, μ and $\kappa^\star, \mu^\star$. The generalized eigenvalue problem (26) then reads*

$$\big[3(\kappa^\star - \Lambda\kappa)\boldsymbol{\mathcal{J}} + 2(\mu^\star - \Lambda\mu)\boldsymbol{\mathcal{K}}\big] : \boldsymbol{E} = \boldsymbol{0}$$

or, using the relations $\boldsymbol{\mathcal{J}} : \boldsymbol{\mathcal{J}} = \boldsymbol{\mathcal{J}}$, $\boldsymbol{\mathcal{K}} : \boldsymbol{\mathcal{K}} = \boldsymbol{\mathcal{K}}$ and $\boldsymbol{\mathcal{J}} : \boldsymbol{\mathcal{K}} = \boldsymbol{0}$ verified by $\boldsymbol{\mathcal{J}}$ and $\boldsymbol{\mathcal{K}}$,

$$(\kappa^\star - \Lambda\kappa)\boldsymbol{\mathcal{J}} : \boldsymbol{E} = \boldsymbol{0} \quad \textit{or} \quad (\mu^\star - \Lambda\mu)\boldsymbol{\mathcal{K}} : \boldsymbol{E} = \boldsymbol{0}.$$

Hence there are two distinct eigenvalues: (i) $\Lambda_1 = \kappa^\star/\kappa$ (multiplicity 1) with eigentensor $\boldsymbol{E}_1 = \boldsymbol{I}$ since $\boldsymbol{\mathcal{J}} : \boldsymbol{E} = (1/3)tr(\boldsymbol{E})\boldsymbol{I}$ for any $\boldsymbol{E} \in \mathbb{R}^{3,3}_{sym}$, and (ii) $\Lambda_2 = \mu^\star/\mu$ (multiplicity 5). Proposition 3 for this case essentially correspond to Theorem 5.4 of **[22]**.

Remark 4. *Proposition 1, together with the inequalities*

$$\boldsymbol{E} : \mathcal{C} : \mathcal{C}^{\star -1} : \Delta\mathcal{C} : \boldsymbol{E} \le \boldsymbol{E} : \boldsymbol{\mathcal{A}} : \boldsymbol{E} \le \boldsymbol{E} : \Delta\mathcal{C} : \boldsymbol{E} \qquad \forall \boldsymbol{E} \in \mathbb{R}^{3,3}_{sym}$$

which imply Proposition 3, constitute Proposition 1 of **[24]**. *Moreover, it is shown in* **[23]** *that (i) positive definiteness of* $\boldsymbol{\mathcal{C}} - \boldsymbol{\mathcal{C}}^\star$ *implies that of* $-\boldsymbol{\mathcal{A}}$ *(Theorem 2.7) and (ii) positive definiteness of* $\boldsymbol{\mathcal{C}}^{-1} - \boldsymbol{\mathcal{C}}^{\star-1}$ *implies that of* $\boldsymbol{\mathcal{A}}$ *(Theorem 2.8). One easily check that cases (i) and (ii) are respectively equivalent to the condition* $\Lambda_I > 1$ $(1 \le I \le 6)$ *or* $\Lambda_I < 1$ $(1 \le I \le 6)$ *of proposition 3.*

A proof of Proposition 3, essentially a concise and self-contained version of the approach used in **[23]** for proving Theorems 2.7 and 2.8 therein, is given for completeness in Appendix A.

3. Asymptotic behavior of the displacement. Finding $\delta(a)$ and the topological derivative $DJ(\boldsymbol{z})$ requires some preliminary results on the small-inhomogeneity asymptotic behavior of $\boldsymbol{u}_a$. To facilitate this task, the transmission problem (12) is first reformulated as a domain integral equation involving a domain integral operator whose support is the small inhomogeneity B_a.

3.1. Elastostatic Green's tensor. Let the elastostatic Green's tensor $\boldsymbol{G}(\boldsymbol{\xi}, \boldsymbol{x})$ be defined by

$$\begin{aligned} &\operatorname{div}\big(\boldsymbol{\mathcal{C}} : \boldsymbol{\varepsilon}[\boldsymbol{G}(\cdot, \boldsymbol{x})]\big) + \delta(\cdot - \boldsymbol{x})\boldsymbol{I} = \boldsymbol{0} \ \text{ in } \Omega, \\ &\qquad\qquad \boldsymbol{G}(\cdot, \boldsymbol{x}) = \boldsymbol{0} \ \text{ on } \Gamma_{\mathrm{D}}, \quad \boldsymbol{t}[\boldsymbol{G}(\cdot, \boldsymbol{x})] = \boldsymbol{0} \ \text{ on } \Gamma_{\mathrm{N}} \qquad (\boldsymbol{x} \in \Omega), \end{aligned} \tag{27}$$

i.e. $\boldsymbol{G}(\cdot, \boldsymbol{x}) = \boldsymbol{e}_k \otimes \boldsymbol{G}^k(\cdot, \boldsymbol{x})$ gathers the three linearly independent elastostatic displacement fields $\boldsymbol{G}^k(\cdot, \boldsymbol{x})$ resulting from unit point forces $\delta(\cdot - \boldsymbol{x})\boldsymbol{e}_k$ applied at $\boldsymbol{x} \in \Omega$ along each coordinate direction k and fulfilling the homogeneous boundary conditions on $\partial\Omega$ implied by the definition of W_0.

Moreover, the ensuing analysis will be facilitated by splitting the elastostatic Green's tensor according to

$$\boldsymbol{G}(\boldsymbol{\xi}, \boldsymbol{x}) = \boldsymbol{G}_\infty(\boldsymbol{\xi} - \boldsymbol{x}) + \boldsymbol{G}_{\mathrm{C}}(\boldsymbol{\xi}, \boldsymbol{x}) \tag{28}$$

where $\boldsymbol{G}_\infty(\boldsymbol{r})$ is the (singular) elastostatic full-space Green's tensor, such that

$$\operatorname{div}\big(\boldsymbol{\mathcal{C}} : \boldsymbol{\varepsilon}[\boldsymbol{G}_\infty]\big) + \delta\boldsymbol{I} = \boldsymbol{0} \quad (\text{in } \mathbb{R}^3), \qquad |\boldsymbol{G}_\infty(\boldsymbol{r})| \to 0 \quad (|\boldsymbol{r}| \to \infty), \tag{29}$$

and the complementary Green's tensor $\boldsymbol{G}_{\mathrm{C}}$ is bounded at $\boldsymbol{\xi} = \boldsymbol{x}$ (and in fact is C^∞ for $\boldsymbol{\xi}, \boldsymbol{x} \in \Omega$ by virtue of being the solution of an elastostatic boundary-value problem with regular boundary data and zero body force density). The full-space Green's tensor is given by the inverse Fourier integral **[36]**

$$\boldsymbol{G}_\infty(\boldsymbol{r}) = \frac{1}{(2\pi)^3} \int_{\mathbb{R}^3} \exp(\mathrm{i}\boldsymbol{\eta}\cdot\boldsymbol{r})\boldsymbol{N}(\boldsymbol{\eta}) \, \mathrm{d}V(\boldsymbol{\eta}) \quad (\boldsymbol{r} \in \mathbb{R}^3 \setminus \{\boldsymbol{0}\}), \tag{30}$$

where, for given $\boldsymbol{\eta} \in \mathbb{R}^3$, the second-order tensor $\boldsymbol{N}(\boldsymbol{\eta})$ is given by $\boldsymbol{N}(\boldsymbol{\eta}) = \boldsymbol{K}^{-1}(\boldsymbol{\eta})$ in terms of the *acoustic tensor* $\boldsymbol{K}(\boldsymbol{\eta})$, defined by $K_{ik}(\boldsymbol{\eta}) = \mathcal{C}_{ijk\ell}\eta_j\eta_\ell$ ($\boldsymbol{K}(\boldsymbol{\eta})$ is invertible for any $\boldsymbol{\eta} \neq \boldsymbol{0}$ and positive definite elasticity tensor $\boldsymbol{\mathcal{C}}$). Moreover, $\boldsymbol{G}_\infty$ has the following homogeneity property, which plays an important role in the sequel:

Lemma 1. $\boldsymbol{G}_\infty$ *is a positively homogeneous tensor-valued function of degree -1. Hence, for any* $\boldsymbol{r} \in \mathbb{R}^3 \setminus \{\boldsymbol{0}\}$ *and* $\lambda \in \mathbb{R} \setminus \{0\}$, $\boldsymbol{G}_\infty$ *and* $\boldsymbol{\nabla}\boldsymbol{G}_\infty$ *verify*

$$\boldsymbol{G}_\infty(\lambda\boldsymbol{r}) = |\lambda|^{-1}\boldsymbol{G}_\infty(\boldsymbol{r}), \qquad \boldsymbol{\nabla}\boldsymbol{G}_\infty(\lambda\boldsymbol{r}) = |\lambda|^{-3}\lambda\boldsymbol{\nabla}\boldsymbol{G}_\infty(\boldsymbol{r}) \tag{31}$$

Proof. Replacing $\boldsymbol{r}$ with $\lambda\boldsymbol{r}$ and performing the change of variable $\boldsymbol{\eta} = \lambda^{-1}\boldsymbol{\eta}'$ in (30), the homogeneity property of $\boldsymbol{G}_\infty$ follows from using (i) $\boldsymbol{N}(\boldsymbol{\eta}) = \lambda^2\boldsymbol{N}(\boldsymbol{\eta}')$ by virtue of $\boldsymbol{K}$ being homogeneous of degree 2 in $\boldsymbol{\eta}$ (and hence $\boldsymbol{N}$ being homogeneous of degree -2), and (ii) $\mathrm{d}V(\boldsymbol{\eta}) = |\lambda|^{-3} \, \mathrm{d}V(\boldsymbol{\eta}')$. □

3.2. Domain integral equation formulation. Lemma 1 implies that both $\boldsymbol{G}(\cdot, \boldsymbol{x})$ and $\boldsymbol{\nabla}\boldsymbol{G}(\cdot, \boldsymbol{x})$ have an integrable singularity at $\boldsymbol{x}$. By virtue of decomposition (28) and the known C^∞ regularity of $\boldsymbol{G}_\infty$ away from the origin, $\boldsymbol{G}(\cdot, \boldsymbol{x})$ hence belongs to $W^{1,1}(\Omega)$. On applying equations (27) in the sense of

distributions for a trial displacement $\boldsymbol{w} \in W_0 \cap C^1(\omega)$ (where ω is a neighbourhood of $\boldsymbol{x}$) and integrating by parts the resulting first term over Ω, the Green's tensor is found to verify the identity

$$\langle \boldsymbol{G}(\cdot,\boldsymbol{x}), \boldsymbol{w} \rangle_\Omega^{\mathcal{C}} = \boldsymbol{w}(\boldsymbol{x}) \qquad \boldsymbol{x} \in \Omega,\ \forall \boldsymbol{w} \in C_c^1(\Omega), \tag{32}$$

whose left-hand side is well-defined. Now, setting $\boldsymbol{w} = \boldsymbol{G}(\cdot,\boldsymbol{x})$ in (12) (noting that the bilinear strain energy integral remains well-defined by virtue of $\boldsymbol{u}$ and $\boldsymbol{v}_a$ having C^1 regularity near $\boldsymbol{x}$ if $\boldsymbol{x} \in B_a \cup (\Omega \setminus \bar{B}_a)$) and using identity (32) with $\boldsymbol{w} = \boldsymbol{v}_a$, the displacement perturbation $\boldsymbol{v}_a$ is found to satisfy

$$\text{Find } \boldsymbol{v}_a \in W_0, \quad \mathcal{L}_a[\boldsymbol{v}_a](\boldsymbol{x}) = -\langle \boldsymbol{u}, \boldsymbol{G}(\cdot,\boldsymbol{x}) \rangle_{B_a}^{\Delta\mathcal{C}}, \quad \forall \boldsymbol{x} \in B_a \cup (\Omega \setminus \bar{B}_a) \tag{33}$$

where the linear integral operator $\mathcal{L}_a$ is defined by

$$\mathcal{L}_a[\boldsymbol{v}](\boldsymbol{x}) = \boldsymbol{v}(\boldsymbol{x}) + \langle \boldsymbol{v}, \boldsymbol{G}(\cdot,\boldsymbol{x}) \rangle_{B_a}^{\Delta\mathcal{C}} \tag{34}$$

Equation (33) is readily recognized as a compactly-written form of the Lippmann-Schwinger domain integral equation governing the elastostatic inhomogeneity problem. If $\boldsymbol{x} \in B_a$, (33) can be solved for $\boldsymbol{v}_a$ inside B_a. Then, if $\boldsymbol{x} \in \Omega \setminus \bar{B}_a$, (33) becomes a representation formula, expressing $\boldsymbol{v}_a$ outside of B_a explicitly knowing $\boldsymbol{v}_a$ inside B_a.

Domain integral equation formulation for the FSTP.. In a similar fashion, the free-space transmission problem (14) can be recast as a domain integral equation by setting $\boldsymbol{w} = \boldsymbol{G}_\infty(\cdot - \boldsymbol{x})$ in (15), to obtain

$$\text{Find } \boldsymbol{v}_{\mathcal{B}} \in W_\infty, \quad \mathcal{L}_{\mathcal{B}}\big[\, \boldsymbol{v}_{\mathcal{B}}[\boldsymbol{E}] \,\big](\boldsymbol{x}) = -\langle \boldsymbol{\varphi}[\boldsymbol{E}], \boldsymbol{G}_\infty(\cdot - \boldsymbol{x}) \rangle_{\mathcal{B}}^{\Delta\mathcal{C}}, \quad \forall \boldsymbol{x} \in \mathcal{B} \cup (\mathbb{R}^3 \setminus \bar{\mathcal{B}}) \tag{35}$$

with the linear integral operator $\mathcal{L}_{\mathcal{B}}$ defined by

$$\mathcal{L}_{\mathcal{B}}[\boldsymbol{v}](\boldsymbol{x}) = \boldsymbol{v}(\boldsymbol{x}) + \langle \boldsymbol{v}, \boldsymbol{G}_\infty(\cdot - \boldsymbol{x}) \rangle_{\mathcal{B}}^{\Delta\mathcal{C}}. \tag{36}$$

The EMT (Sec. 2.4) then manifests itself naturally when considering the far-field behavior of $\boldsymbol{v}_{\mathcal{B}}[\boldsymbol{E}]$. Indeed, from (35), $\boldsymbol{v}_{\mathcal{B}}[\boldsymbol{E}](\bar{\boldsymbol{x}})$ is given, for $\bar{\boldsymbol{x}} \notin \bar{\mathcal{B}}$, by the representation formula

$$\boldsymbol{v}_{\mathcal{B}}[\boldsymbol{E}](\bar{\boldsymbol{x}}) = -\int_{\mathcal{B}} \boldsymbol{\nabla}\boldsymbol{G}_\infty(\cdot - \bar{\boldsymbol{x}}) : \Delta\boldsymbol{\mathcal{C}} : (\boldsymbol{E} + \boldsymbol{\nabla}\boldsymbol{v}_{\mathcal{B}}[\boldsymbol{E}])\, \mathrm{d}V \tag{37}$$

(having used $\boldsymbol{\nabla}\boldsymbol{\varphi}[\boldsymbol{E}] = \boldsymbol{E}$). Applying a Taylor expansion to $\boldsymbol{\nabla}\boldsymbol{G}_\infty(\bar{\boldsymbol{\xi}} - \bar{\boldsymbol{x}})$ about $\bar{\boldsymbol{\xi}} = \boldsymbol{0}$ and invoking the homogeneity property (31) yields $\boldsymbol{\nabla}\boldsymbol{G}_\infty(\bar{\boldsymbol{\xi}} - \bar{\boldsymbol{x}}) = -\boldsymbol{\nabla}\boldsymbol{G}_\infty(\bar{\boldsymbol{x}}) + O(|\boldsymbol{x}|^{-3})$ ($|\boldsymbol{x}| \to +\infty$). Consequently, the far-field behavior of $\boldsymbol{v}_{\mathcal{B}}[\boldsymbol{E}](\boldsymbol{x})$ as given by (37) is obtained as

$$\boldsymbol{v}_{\mathcal{B}}[\boldsymbol{E}](\boldsymbol{x}) = -\boldsymbol{\nabla}\boldsymbol{G}_\infty(\boldsymbol{x}) : \boldsymbol{\mathcal{A}} : \boldsymbol{E} + O(|\boldsymbol{x}|^{-3}) \qquad (|\boldsymbol{x}| \to +\infty) \tag{38}$$

3.3. Asymptotic behavior of $\boldsymbol{v}_a$. The leading asymptotic behavior of $\boldsymbol{v}_a$ is now investigated, which naturally leads to seek the limiting form for $a \to 0$ of integral equation (33). Moreover, since equation (33) involves integrals over the vanishing inhomogeneity B_a, it is convenient to rescale points $\boldsymbol{\xi}, \boldsymbol{x} \in B_a$, and consequently the differential volume element, according to:

$$\text{(a) } (\boldsymbol{\xi}, \boldsymbol{x}) = \boldsymbol{z} + a(\bar{\boldsymbol{\xi}}, \bar{\boldsymbol{x}}), \qquad \text{(b) } \mathrm{d}V_\xi = a^3\, \mathrm{d}\bar{V}_{\bar{\xi}} \qquad (\boldsymbol{\xi} \in B_a,\ \bar{\boldsymbol{\xi}} \in \mathcal{B}). \tag{39}$$

This scaling is then introduced into (33). Invoking the decomposition (28) of $\boldsymbol{G}(\boldsymbol{\xi}, \boldsymbol{x})$, the homogeneity property (31) and the boundedness of $\boldsymbol{G}_{\mathrm{C}}$ in B_a, one has

$$\boldsymbol{\nabla}_1\boldsymbol{G}(\boldsymbol{\xi}, \boldsymbol{x}) = a^{-2}\boldsymbol{\nabla}\boldsymbol{G}_\infty(\bar{\boldsymbol{\xi}} - \bar{\boldsymbol{x}}) + \boldsymbol{\nabla}_1\boldsymbol{G}_{\mathrm{C}}(\boldsymbol{z}, \boldsymbol{z}) + o(1) \tag{40}$$

Moreover, introducing the rescaled coordinates (39a) into $\boldsymbol{v}_a$ and $\boldsymbol{u}$ and setting $\bar{\boldsymbol{v}}_a(\bar{\boldsymbol{\xi}}) := \boldsymbol{v}_a(\boldsymbol{z} + a\bar{\boldsymbol{\xi}})$, one obtains $\boldsymbol{\nabla}\boldsymbol{v}_a(\boldsymbol{\xi}) = a^{-1}\boldsymbol{\nabla}\bar{\boldsymbol{v}}_a(\bar{\boldsymbol{\xi}})$ and $\boldsymbol{\nabla}\boldsymbol{u}(\boldsymbol{\xi}) = \boldsymbol{\nabla}\boldsymbol{u}(\boldsymbol{z}) + O(a)$. Using these expansions, together with (40) and (39b), in both sides of equation (33) then yields the expansions

$$\begin{aligned}
\mathcal{L}_a[\boldsymbol{v}_a](\boldsymbol{x}) &= \bar{\boldsymbol{v}}_a(\bar{\boldsymbol{x}}) + \langle \bar{\boldsymbol{v}}_a, \boldsymbol{G}_\infty(\cdot, \bar{\boldsymbol{x}}) \rangle_{\mathcal{B}}^{\Delta\mathcal{C}} + O\big(a^2 \|\boldsymbol{\nabla}\bar{\boldsymbol{v}}_a\|_{L^2(\mathcal{B})}\big) + o(\|\boldsymbol{\nabla}\bar{\boldsymbol{v}}_a\|_{L^2(\mathcal{B})}) \\
&= \mathcal{L}_{\mathcal{B}}[\bar{\boldsymbol{v}}_a](\bar{\boldsymbol{x}}) + o(\|\boldsymbol{\nabla}\bar{\boldsymbol{v}}_a\|_{L^2(\mathcal{B})}) \\
\langle \boldsymbol{u}, \boldsymbol{G}(\cdot,\boldsymbol{x}) \rangle_{B_a}^{\Delta\mathcal{C}} &= a\langle \boldsymbol{\varphi}[\boldsymbol{\nabla}\boldsymbol{u}(\boldsymbol{z})], \boldsymbol{G}_\infty(\cdot, \bar{\boldsymbol{x}}) \rangle_{\mathcal{B}}^{\Delta\mathcal{C}} + o(a).
\end{aligned}$$

By virtue of the above expansions, the integral equation resulting from retaining only the contributions of lowest order in a in (33) is thus found to coincide with the integral equation (35) governing the free-space transmission problem with $\boldsymbol{E} = a\boldsymbol{\nabla u}(\boldsymbol{z})$. This suggests setting $\boldsymbol{v}_a$ in the form

$$\boldsymbol{v}_a(\boldsymbol{x}) = a\boldsymbol{v}_{\mathcal{B}}[\boldsymbol{\nabla u}(\boldsymbol{z})]\Big(\frac{\boldsymbol{x}-\boldsymbol{z}}{a}\Big) + \boldsymbol{\delta}_a(\boldsymbol{x}) \qquad \boldsymbol{x} \in B_a$$

The function $a\boldsymbol{v}_{\mathcal{B}}[\boldsymbol{\nabla u}(\boldsymbol{z})]\big((\boldsymbol{x}-\boldsymbol{z})/a\big)$ indeed defines the leading contribution to the so-called inner expansion of $\boldsymbol{v}_a$, with the remainder $\boldsymbol{\delta}_a$ only contributing higher order terms in the limit $a \to 0$, as stated in the following Proposition, whose proof is deferred to Appendix 4.

Proposition 4 (asymptotic behavior of $\boldsymbol{v}_a$)**.** *Let the inner approximation $\tilde{\boldsymbol{v}}_a$ to $\boldsymbol{v}_a$ be defined by*

$$\tilde{\boldsymbol{v}}_a(\boldsymbol{x}) = a\boldsymbol{v}_{\mathcal{B}}[\boldsymbol{\nabla u}(\boldsymbol{z})]\Big(\frac{\boldsymbol{x}-\boldsymbol{z}}{a}\Big), \qquad \boldsymbol{x} \in B_a \tag{41}$$

where $\boldsymbol{v}_{\mathcal{B}}[\boldsymbol{\nabla u}(\boldsymbol{z})]$ solves the FSTP (15) *with $\boldsymbol{E} = \boldsymbol{\nabla u}(\boldsymbol{z})$. Moreover, for any cut-off function $\theta \in C_c^\infty(\Omega)$ such that $\theta \equiv 1$ in a neighborhood D of $\boldsymbol{z}$, let $\boldsymbol{\delta}_a \in H^1(\Omega;\mathbb{R}^3)$ be defined by*

$$\boldsymbol{v}_a = \theta\tilde{\boldsymbol{v}}_a + \boldsymbol{\delta}_a \tag{42}$$

Assume also that $\boldsymbol{f}$ has $C^{0,\beta}$ regularity for some $\beta > 0$ in a neighbourhood of $\boldsymbol{z}$. Then there exists a constant $C > 0$ independent of a such that

$$\|\boldsymbol{\delta}_a\|_{H^1(\Omega)} \leq Ca^{5/2}. \tag{43}$$

Moreover

$$\|\tilde{\boldsymbol{v}}_a\|_{L^2(\Omega)} \leq Ca^{5/2} \quad \text{and} \quad \|\boldsymbol{\nabla}\tilde{\boldsymbol{v}}_a\|_{L^2(\Omega)} \leq Ca^{3/2}. \tag{44}$$

Remark 5. *The formulation and proof of Proposition 4, in particular regarding the introduction of $\boldsymbol{\delta}_a$ as defined by* (42)*, follow the approach of* **[37]***. As also remarked in* **[37]***, $\tilde{\boldsymbol{v}}_a$ provides the leading contribution to the inner expansion of $\boldsymbol{v}_a$ in the sense that (i) $\theta = 1$ in B_a and can be made to vanish outside of an arbitrarily small neighbourhood of B_a and (ii) $\|\boldsymbol{\nabla}\boldsymbol{\delta}_a\|_{L^2(\Omega)} = O(a^{5/2})$ while $\|\boldsymbol{\nabla}\tilde{\boldsymbol{v}}_a\|_{L^2(\Omega)} = O(a^{3/2})$.*

Remark 6. *Proposition 4, established assuming $\boldsymbol{\mathcal{C}}$ to be constant (homogeneous background material), is expected to also hold for heterogeneous elastic properties that are smooth in a fixed neighbourhood of $\boldsymbol{z}$ (with the EMT then defined in terms of $\boldsymbol{\mathcal{C}}(\boldsymbol{z})$). Both* **[13]** *for the electrostatic case and* **[24]** *for the elastic case assume smooth heterogeneous background properties in Ω, the former emphasizing that the assumption may be significantly weakened.*

Remark 7. *Expansion (42) is the specialization to diametrically-small inhomogeneities of expansions obtained by* **[24]** *for more general classes of anisotropic inhomogeneities with vanishing measure $|B_a|$ (e.g. thin or elongated inhomogeneities).*

4. Topological expansion of cost functionals.

4.1. Small inhomogeneity of arbitrary shape. To establish an expansion of the form (18) of $J(\boldsymbol{\mathcal{C}}_a)$ with the help of Proposition 4, the first step exploits a first-order Taylor expansion of the densities ψ_Ω, ψ_Γ of (16), to obtain

$$J(\boldsymbol{\mathcal{C}}_a) = J(\boldsymbol{\mathcal{C}}) + \mathbb{J}'(\boldsymbol{u};\boldsymbol{v}_a) + \mathbb{J}_{\mathrm{R}}(\boldsymbol{u};\boldsymbol{v}_a) \tag{45}$$

where $\mathbb{J}'(\boldsymbol{u};\boldsymbol{w})$ is the directional derivative of $\mathbb{J}$ at $\boldsymbol{u}$ in the direction $\boldsymbol{w} \in W_0$, i.e.

$$\mathbb{J}'(\boldsymbol{u};\boldsymbol{w}) = \int_\Omega \psi'_\Omega(\cdot,\boldsymbol{u})\cdot\boldsymbol{w}\,\mathrm{d}V + \int_{\Gamma_{\mathrm{N}}} \psi'_\Gamma(\cdot,\boldsymbol{u})\cdot\boldsymbol{w}\,\mathrm{d}S \tag{46}$$

and the remainder $\mathbb{J}_{\mathrm{R}}(\boldsymbol{u};\boldsymbol{v}_a)$ can be expressed in the form

$$\mathbb{J}_{\mathrm{R}}(\boldsymbol{u};\boldsymbol{v}_a) = \tfrac{1}{2}\int_\Omega \boldsymbol{v}_a\cdot\psi''_\Omega(\cdot,\boldsymbol{u}+t_\Omega\boldsymbol{v}_a)\cdot\boldsymbol{v}_a\,\mathrm{d}V + \int_{\Gamma_{\mathrm{N}}} \boldsymbol{v}_a\cdot\psi''_\Gamma(\cdot,\boldsymbol{u}+t_\Gamma\boldsymbol{v}_a)\cdot\boldsymbol{v}_a\,\mathrm{d}S \tag{47}$$

for some $t_\Omega, t_\Gamma \in [0,1]$. Since $\boldsymbol{v}_a \in W_0$ for any a, the support of the boundary integrals in (46) and (47) is reduced to Γ_N. The topological derivative of $J(\boldsymbol{\mathcal{C}}_a)$ is the leading contribution as $a \to 0$ of expansion (45), and will be found by estimating the directional derivative (46) and the remainder (47).

First, by virtue of the growth conditions (17) on ψ_Ω and ψ_Γ, the remainder (47) can be bounded, for some positive constant C, as

$$\mathbb{J}_\mathrm{R}(\boldsymbol{u};\boldsymbol{v}_a) \leq C\big[\,\|\boldsymbol{v}_a\|^2_{L^2(\Omega)} + \|\boldsymbol{v}_a\|^2_{L^2(\Gamma_\mathrm{N})}\,\big]$$

Invoking estimates (43) and (44), one has

$$\|\boldsymbol{v}_a\|^2_{L^2(\Omega)} \leq \|\boldsymbol{v}_a\|^2_{H^1(\Omega)} = \|\theta\tilde{\boldsymbol{v}}_a + \boldsymbol{\delta}_a\|^2_{H^1(\Omega)} \leq Ca^5,$$

while, since $\boldsymbol{v}_a = \boldsymbol{\delta}_a$ on Γ_N, one also has (again invoking (43))

$$\|\boldsymbol{v}_a\|^2_{L^2(\Gamma_\mathrm{N})} = \|\boldsymbol{\delta}_a\|^2_{L^2(\Gamma_\mathrm{N})} \leq \|\boldsymbol{\delta}_a\|^2_{H^1(\Omega)} \leq Ca^5.$$

(in fact, one can show from (33) used for $\boldsymbol{x} \in \Gamma_\mathrm{N}$ that $\|\boldsymbol{v}_a\|^2_{L^2(\Gamma_\mathrm{N})} \leq Ca^6$). As a result, one obtains

$$\mathbb{J}_\mathrm{R}(\boldsymbol{u};\boldsymbol{v}_a) \leq Ca^5 \tag{48}$$

The directional derivative $\mathbb{J}'(\boldsymbol{u};\boldsymbol{v}_a)$ remains to be evaluated. To this aim, it is convenient to introduce the adjoint solution $\boldsymbol{p}$ defined by the weak formulation

$$\text{Find } \boldsymbol{p} \in W_0, \qquad \langle \boldsymbol{p}, \boldsymbol{w}\rangle^{\mathcal{C}}_\Omega = \mathbb{J}'(\boldsymbol{u};\boldsymbol{w}), \quad \forall \boldsymbol{w} \in W_0, \tag{49}$$

Then, on setting $\boldsymbol{w} = \boldsymbol{p}$ in (12) and $\boldsymbol{w} = \boldsymbol{v}_a$ in (49), combining the resulting identities and exploiting the symmetry of the energy bilinear form, one obtains

$$\mathbb{J}'(\boldsymbol{u};\boldsymbol{v}_a) = -\langle \boldsymbol{p}, \boldsymbol{u}\rangle^{\Delta\mathcal{C}}_{B_a} - \langle \boldsymbol{p}, \boldsymbol{v}_a\rangle^{\Delta\mathcal{C}}_{B_a} = -\langle \boldsymbol{p}, \boldsymbol{u}_a\rangle^{\Delta\mathcal{C}}_{B_a} \tag{50}$$

The above equation shows that the asymptotic behavior of $\mathbb{J}'(\boldsymbol{u};\boldsymbol{v}_a)$ as $a \to 0$ can be determined from the inner asymptotic behavior of $\boldsymbol{v}_a$, which is given by (42). This is achieved by the following lemma:

Lemma 2. *For any vector field $\boldsymbol{w} \in C^2(D;\mathbb{R}^3)$, where $D \subset \Omega$ is a neighbourhood of B_a, one has*

$$\langle \boldsymbol{w}, \boldsymbol{u}_a\rangle^{\Delta\mathcal{C}}_{B_a} = a^3 \boldsymbol{\nabla}\boldsymbol{w}(\boldsymbol{z}) : \boldsymbol{\mathcal{A}} : \boldsymbol{\nabla}\boldsymbol{u}(\boldsymbol{z}) + o(a^3) \tag{51}$$

where $\boldsymbol{\mathcal{A}}$ is the elastic moment tensor defined by (19).

Proof. See proof of Proposition 5 below. □

Under the requirements made on ψ_Ω in Sec. 2.3 and the additional assumption that $\psi'_\Omega(\cdot,\boldsymbol{u})$ have $C^{0,\beta}(V)$ regularity for some $\beta > 0$ in a neighbourhood V of $\boldsymbol{z}$, the solution $\boldsymbol{p}$ of (49) is in $C^2(V;\mathbb{R}^3)$. Application of Lemma 2 with $\boldsymbol{w} = \boldsymbol{p}$ to (50) gives

$$\mathbb{J}'(\boldsymbol{u};\boldsymbol{v}_a) = -a^3 \boldsymbol{\nabla}\boldsymbol{p}(\boldsymbol{z}) : \boldsymbol{\mathcal{A}} : \boldsymbol{\nabla}\boldsymbol{u}(\boldsymbol{z}) + o(a^3). \tag{52}$$

On using estimates (48) and (52) in (45) and comparing the resulting expansion with (18), the asymptotic behavior $\delta(a)$ and the topological derivative $DJ(\boldsymbol{z})$ of J are as stated next:

Proposition 5 (topological derivative of J)**.** *Assume that ψ_Ω satisfies the requirements made in Sec. 2.3, and that $\psi'_\Omega(\cdot,\boldsymbol{u})$ have $C^{0,\beta}$ regularity for some $\beta > 0$ in a neighbourhood of $\boldsymbol{z}$. The topological derivative $DJ(\boldsymbol{z})$ of $J(\boldsymbol{\mathcal{C}}_a)$ at $\boldsymbol{z}$ and its asymptotic behavior $\delta(a)$ are given by*

$$DJ(\boldsymbol{z}) = -\boldsymbol{\nabla}\boldsymbol{u}(\boldsymbol{z}) : \boldsymbol{\mathcal{A}} : \boldsymbol{\nabla}\boldsymbol{p}(\boldsymbol{z}), \qquad \delta(a) = a^3, \tag{53}$$

where the background field $\boldsymbol{u}$ and the adjoint field $\boldsymbol{p}$ solve (3) *and* (49)*, respectively, and $\boldsymbol{\mathcal{A}}$ is the elastic moment tensor defined by* (2.4)*.*

Proof. The proposition only requires a proof for Lemma 2. To this aim, one notes that the following expansion is available for $\boldsymbol{\nabla w}$:

$$\boldsymbol{\nabla w}(\boldsymbol{\xi}) = \boldsymbol{\nabla w}(\boldsymbol{z}) + O(|\boldsymbol{\xi}-\boldsymbol{z}|) = \boldsymbol{\nabla w}(\boldsymbol{z}) + O(a|\bar{\boldsymbol{\xi}}|) \quad (\boldsymbol{\xi}\in B_a).$$

Moreover, a similar expansion is available for $\boldsymbol{u}$, while (42) yields

$$\boldsymbol{\nabla v}_a(\boldsymbol{\xi}) = \boldsymbol{\nabla v}_{\mathcal{B}}[\boldsymbol{\nabla u}(\boldsymbol{z})](\bar{\boldsymbol{\xi}}) + \boldsymbol{\nabla \delta}_a(\boldsymbol{\xi}) \quad (\boldsymbol{\xi}\in B_a, \bar{\boldsymbol{\xi}}\in\mathcal{B}).$$

Using the above expansions and rescaling (39), one obtains

$$\begin{aligned}\langle \boldsymbol{w}, \boldsymbol{u}_a\rangle_{B_a}^{\Delta\mathcal{C}} &= a^3 \boldsymbol{\nabla w}(\boldsymbol{z}) : \Big\{ \int_{\mathcal{B}} \Delta\boldsymbol{\mathcal{C}} : \big(\boldsymbol{\nabla u}(\boldsymbol{z}) + \boldsymbol{\nabla v}_{\mathcal{B}}[\boldsymbol{\nabla u}(\boldsymbol{z})](\bar{\boldsymbol{\xi}})\big)\, \mathrm{d}\bar{V}_{\bar{\xi}} \Big\} + \langle \boldsymbol{w}, \boldsymbol{\delta}_a\rangle_{B_a}^{\Delta\mathcal{C}} + O(a^4) \\ &= a^3 \boldsymbol{\nabla w}(\boldsymbol{z}) : \boldsymbol{\mathcal{A}} : \boldsymbol{\nabla u}(\boldsymbol{z}) + \langle \boldsymbol{w}, \boldsymbol{\delta}_a\rangle_{B_a}^{\Delta\mathcal{C}} + O(a^4)\end{aligned}$$

using definition (19) of the EMT. Finally, the estimate

$$\langle \boldsymbol{w}, \boldsymbol{\delta}_a\rangle_{B_a}^{\Delta\mathcal{C}} \le C\|\boldsymbol{\varepsilon}[\boldsymbol{w}]\|_{L^2(B_a)}\|\boldsymbol{\varepsilon}[\boldsymbol{\delta}_a]\|_{L^2(B_a)} \le Ca^{3/2}\|\boldsymbol{\delta}_a\|_{H^1(\Omega)} \le Ca^{3/2}a^{5/2} = Ca^4 = o(a^3)$$

holds for some constant C by virtue of (43). This completes the proof. □

Remark 8. *The analysis leading to Proposition 5 does not apply in the case of small inhomogeneities nucleating at the boundary, i.e. if $\boldsymbol{z}\in\partial\Omega$. To address this case, the free-space transmission problem should be replaced with a half-space transmission problem for a normalized inhomogeneity intersecting the traction-free planar surface; likewise $\boldsymbol{G}_\infty$ has to be replaced with the fundamental solution for the half-space. Available references on asymptotic methods for small surface-breaking defects are much scarcer than for internal defects, see e.g.* **[38, 39, 40]**.

Remark 9. *The foregoing analysis, and in particular Proposition 5, still holds if the cost functional format* (16) *is extended to also allow integrals of the form*

$$\int_S \psi_S(\boldsymbol{\xi}, \boldsymbol{w})\, dS(\boldsymbol{\xi})$$

where $S\subset\bar{\Omega}$ is an arbitrary surface, provided $DJ(\boldsymbol{z})$ is evaluated at points $\boldsymbol{z}\notin S$

Remark 10 (topological derivative of potential energy)**.** *For the special case of the potential energy* (11) *with $\bar{\boldsymbol{u}}=\boldsymbol{0}$, one has $\mathbb{J}'(\boldsymbol{u},\boldsymbol{w}) = -(1/2)F(\boldsymbol{w})$. Hence, $\boldsymbol{p} = -(1/2)\boldsymbol{u}$ and* (53) *yields*

$$DJ_{pot}(\boldsymbol{z}) = \tfrac{1}{2}\boldsymbol{\nabla u}(\boldsymbol{z}) : \boldsymbol{\mathcal{A}} : \boldsymbol{\nabla u}(\boldsymbol{z}). \tag{54}$$

4.2. Small inhomogeneity of ellipsoidal shape. The practical evaluation of DJ requires that of the elastic moment tensor, which is given for an arbitrary inhomogeneity shape $\mathcal{B}$ by (19) in terms of six FSTP solutions (15).

When $\mathcal{B}$ is an ellipsoid, problem (15) has a known analytical solution $\boldsymbol{v}_{\mathcal{B}}[\boldsymbol{E}]$ whose strain is uniform inside $\mathcal{B}$ **[34]**. This solution can be established by means of the equivalent inclusion method **[36]**, briefly recalled in Appendix C, to obtain:

$$\boldsymbol{\varepsilon}[\boldsymbol{v}_{\mathcal{B}}[\boldsymbol{E}]] = -\boldsymbol{\mathcal{S}} : (\boldsymbol{\mathcal{C}} + \Delta\boldsymbol{\mathcal{C}} : \boldsymbol{\mathcal{S}})^{-1} : \Delta\boldsymbol{\mathcal{C}} : \boldsymbol{E}. \tag{55}$$

In (55), $\boldsymbol{\mathcal{S}} = \boldsymbol{\mathcal{S}}(\mathcal{B}, \boldsymbol{\mathcal{C}})$ denotes the (fourth-order) Eshelby tensor, which depends only on $\mathcal{B}$ and $\boldsymbol{\mathcal{C}}$. Its Cartesian components in an orthonormal frame $(\boldsymbol{e}_1, \boldsymbol{e}_2, \boldsymbol{e}_3)$ aligned with the principal directions of $\mathcal{B}$ are given in the general anisotropic case by ([**36**], eq. (17.19))

$$\mathcal{S}_{ijk\ell} = \frac{1}{8\pi}\mathcal{C}_{mnk\ell}\int_\Sigma \big[\eta_j N_{im}(\boldsymbol{\eta}) + \eta_i N_{jm}(\boldsymbol{\eta})\big]\eta_n \,\mathrm{d}\Sigma(\hat{\boldsymbol{\eta}}), \tag{56}$$

where $\Sigma := \{\hat{\boldsymbol{\eta}}\in\mathbb{R}^3,\ |\hat{\boldsymbol{\eta}}|=1\}$ is the unit sphere, $\boldsymbol{\eta} := a_1^{-1}\hat{\eta}_1\boldsymbol{e}_1 + a_2^{-1}\hat{\eta}_2\boldsymbol{e}_2 + a_3^{-1}\hat{\eta}_3\boldsymbol{e}_3$ (where a_1, a_2, a_3 are the principal semiaxes of $\mathcal{B}$) and $\boldsymbol{N}(\boldsymbol{\eta})$ is defined as in (30). Note that (56) has been expressed as

an integral over the unit sphere by effecting on eq. (17.19) of **[36]** the transformation $u = \cos\phi$ with $\phi \in [0, \pi]$.

For an arbitrary anisotropic background, evaluation of (56) requires numerical quadrature (see Sec. 6, and also the more complete treatment of **[41]**), while analytical formulae involving elliptic integrals are available for isotropic background materials **[36]**. The latter reduce to the following elementary closed-form expression when $\mathcal{B}$ is a ball:

$$\boldsymbol{\mathcal{S}} = S_1 \boldsymbol{\mathcal{J}} + S_2 \boldsymbol{\mathcal{K}}, \qquad \text{with} \quad S_1 := \frac{1+\nu}{3(1-\nu)}, \;\; S_2 := \frac{8-10\nu}{15(1-\nu)}, \tag{57}$$

where $\boldsymbol{\mathcal{J}}$ and $\boldsymbol{\mathcal{K}}$ are defined as in (7) and $\nu := (3\kappa - 2\mu)/(6\kappa + 2\mu)$ is Poisson's ratio. The Eshelby tensor $\boldsymbol{\mathcal{S}}$ has the minor symmetries $\mathcal{S}_{ijk\ell} = \mathcal{S}_{jik\ell} = \mathcal{S}_{ij\ell k}$, as is evident from (56). The major symmetry $\mathcal{S}_{ijk\ell} = \mathcal{S}_{k\ell ij}$ holds for the special case (57) but is not true in general.

With the help of (55), the value of $\boldsymbol{\mathcal{A}}$ is then found as follows:

Proposition 6 (elastic moment tensor for an ellipsoidal inhomogeneity)**.** *The elastic moment tensor $\boldsymbol{\mathcal{A}}$ associated with an ellipsoidal inhomogeneity $(\mathcal{B}, \boldsymbol{\mathcal{C}} + \Delta\boldsymbol{\mathcal{C}})$ embedded in a medium with elasticity tensor $\boldsymbol{\mathcal{C}}$ is given by*

$$\boldsymbol{\mathcal{A}} = |\mathcal{B}| \boldsymbol{\mathcal{C}} : (\boldsymbol{\mathcal{C}} + \Delta\boldsymbol{\mathcal{C}} : \boldsymbol{\mathcal{S}})^{-1} : \Delta\boldsymbol{\mathcal{C}} \tag{58}$$

Proof. On using expression (55) of $\boldsymbol{\varepsilon}[\boldsymbol{v}_{\mathcal{B}}]$ in (19) and using the fact that the integrand in the resulting formula is constant, one obtains

$$\boldsymbol{E}' : \boldsymbol{\mathcal{A}} : \boldsymbol{E} = |\mathcal{B}| \big(\boldsymbol{E}' : \Delta\boldsymbol{\mathcal{C}} : \boldsymbol{E} - \boldsymbol{E}' : \Delta\boldsymbol{\mathcal{C}} : \boldsymbol{\mathcal{S}} : (\boldsymbol{\mathcal{C}} + \Delta\boldsymbol{\mathcal{C}} : \boldsymbol{\mathcal{S}})^{-1} : \Delta\boldsymbol{\mathcal{C}} : \boldsymbol{E} \big)$$

Then, since the above equality holds for any constant tensors $\boldsymbol{E}', \boldsymbol{E}$, the sought expression (58) is readily obtained by invoking the identity $\Delta\boldsymbol{\mathcal{C}} : \boldsymbol{\mathcal{S}} : (\boldsymbol{\mathcal{C}} + \Delta\boldsymbol{\mathcal{C}} : \boldsymbol{\mathcal{S}})^{-1} = \boldsymbol{\mathcal{I}} - \boldsymbol{\mathcal{C}} : (\boldsymbol{\mathcal{C}} + \Delta\boldsymbol{\mathcal{C}} : \boldsymbol{\mathcal{S}})^{-1}$. □

Spherical isotropic inhomogeneity, isotropic background. In this case, $\boldsymbol{\mathcal{A}}$ admits a quite simple explicit expression. Using that $\boldsymbol{\mathcal{C}}$ and $\boldsymbol{\mathcal{C}}^\star$ are of the form (7) with respective moduli pairs κ, μ and $\kappa^\star, \mu^\star$ and $\boldsymbol{\mathcal{S}}$ is given by (57), invoking the relations $\boldsymbol{\mathcal{J}} : \boldsymbol{\mathcal{J}} = \boldsymbol{\mathcal{J}}$, $\boldsymbol{\mathcal{K}} : \boldsymbol{\mathcal{K}} = \boldsymbol{\mathcal{K}}$ and $\boldsymbol{\mathcal{J}} : \boldsymbol{\mathcal{K}} = \boldsymbol{0}$ verified by $\boldsymbol{\mathcal{J}}$ and $\boldsymbol{\mathcal{K}}$ and noting in particular that $(A\boldsymbol{\mathcal{J}} + B\boldsymbol{\mathcal{K}})^{-1} = A^{-1}\boldsymbol{\mathcal{J}} + B^{-1}\boldsymbol{\mathcal{K}}$ for any $(A, B) \neq (0, 0)$, one easily evaluates (58) to obtain

$$\boldsymbol{\mathcal{A}} = \frac{4\pi}{3} \left[3\kappa \frac{\Lambda_1 - 1}{1 + S_1(\Lambda_1 - 1)} \boldsymbol{\mathcal{J}} + 2\mu \frac{\Lambda_2 - 1}{1 + S_2(\Lambda_2 - 1)} \boldsymbol{\mathcal{K}} \right] \tag{59}$$

(with $\Lambda_1 := \kappa^\star/\kappa$, $\Lambda_2 := \mu^\star/\mu$). For $0 \leq \nu \leq 0.5$ one has $1/3 \leq S_1 \leq 1$ and $8/15 \geq S_2 \geq 2/5$; combined with $\Lambda_{1,2} \geq 0$. This implies that both denominators in (59) are strictly positive, ensuring in particular the invertibility of $\boldsymbol{\mathcal{C}} + \Delta\boldsymbol{\mathcal{C}} : \boldsymbol{\mathcal{S}}$ upon which (59) depends, except for the special case $\nu = 0.5$, $\kappa^\star = 0$.

4.3. The plane strain case. The derivation of $DJ(\boldsymbol{z})$ under two-dimensional, plane strain, conditions repeats that of Secs. 3 and 4.1, the main modifications being that (i) in (30), $\boldsymbol{N}(\boldsymbol{\eta})$ is now defined in terms of the two-dimensional version of $\boldsymbol{K}(\boldsymbol{\eta})$ (i.e. $K_{ik} = \mathcal{C}_{ijk\ell}\eta_j\eta_\ell$ with $1 \leq i, j, k, \ell \leq 2$) and the multiplicative factor in front of the integral becomes $(2\pi)^{-2}$, and (ii) volume scaling (39b) becomes $\mathrm{d}V_\xi = a^2 \, \mathrm{d}\bar{V}_{\bar{\xi}}$. In particular, $\boldsymbol{\nabla}\boldsymbol{G}_\infty(\boldsymbol{r})$ is now homogeneous of degree -1 in $\boldsymbol{r}$.

As a result, the form (42) of the inner expansion of $\boldsymbol{v}_a$ is still valid, the asymptotic behavior of $J(\boldsymbol{\mathcal{C}}_a)$ in (18) is now given by $\delta(a) = a^2$, and $DJ(\boldsymbol{z})$ remains given by (53).

Of course, the normalized inhomogeneity shape $\mathcal{B}$ involved in the FSTP solution entering definition (19) of $\boldsymbol{\mathcal{A}}$ is now two-dimensional. When $\mathcal{B}$ is an ellipse, expression (58) requires the plane-strain counterpart of the Eshelby tensor $\boldsymbol{\mathcal{S}}$, which is given by

$$\mathcal{S}_{ijk\ell} = \frac{1}{4\pi} \mathcal{C}_{mnk\ell} \int_0^{2\pi} \big[\alpha_i(\theta) N_{jm}\big(\boldsymbol{\alpha}(\theta)\big) + \alpha_j(\theta) N_{im}\big(\boldsymbol{\alpha}(\theta)\big) \big] \alpha_n(\theta) \, \mathrm{d}\theta \tag{60}$$

with $\boldsymbol{\alpha}(\theta)$ defined by

$$\boldsymbol{\alpha}(\theta) = a_1^{-1} \cos\theta \, \boldsymbol{e}_1 + a_2^{-1} \sin\theta \, \boldsymbol{e}_2$$

Formula (60) is established by considering, in the three-dimensional expression (56), the limiting case $a_3 \to \infty$ where the ellipsoid $\mathcal{B}$ approaches a cylinder of axis $\boldsymbol{e}_3$ and elliptic cross-section in the $(\boldsymbol{e}_1, \boldsymbol{e}_2)$-plane. In that case, setting $(\cos\theta, \sin\theta) := (\hat{\eta}_1^2 + \hat{\eta}_2^2)^{-1/2}(\hat{\eta}_1, \hat{\eta}_2)$, one has $\boldsymbol{\eta} = (\hat{\eta}_1^2 + \hat{\eta}_2^2)^{1/2}\boldsymbol{\alpha}(\theta) + O(a_3^{-1})$, which (due to $\boldsymbol{\eta} \longmapsto \boldsymbol{N}(\boldsymbol{\eta})$ being homogeneous of degree -2) implies that

$$\boldsymbol{\eta} \otimes \boldsymbol{N}\big(\boldsymbol{\eta}\big) \otimes \boldsymbol{\eta} = \boldsymbol{\alpha}(\theta) \otimes \boldsymbol{N}\big(\boldsymbol{\alpha}(\theta)\big) \otimes \boldsymbol{\alpha}(\theta) + o(1) \qquad (a_3 \to \infty)$$

Setting $\mathrm{d}\Sigma = \sin\phi \, \mathrm{d}\phi \, \mathrm{d}\theta$ in (56), the integration w.r.t. $\phi \in [0, \pi]$ becomes trivial, with (56) reducing to (60) as a result.

Remark 11. *The existence of plane strain deformations in anisotropic elastic solids is subject to restrictions on $\boldsymbol{\mathcal{C}}$, see e.g.* **[42]**. *All materials having $x_3 = 0$ as material symmetry plane (known as monoclinic materials, and featuring up to 13 independent elastic moduli) permit plane strain states in the (x_1, x_2) plane.*

Isotropic inhomogeneity and background. For this case, analytical evaluation of (60) yields the following explicit expression of $\boldsymbol{\mathcal{S}}$, which coincides with formulae (11.22) of **[36]** given for the ellipsoid infinitely elongated along the x_3 direction:

$$\begin{aligned} \mathcal{S}_{1111} &= A(1-m)(3+\gamma+m) & \mathcal{S}_{1122} &= A(1-m)(1-\gamma-m) \\ \mathcal{S}_{2211} &= A(1+m)(3+\gamma-m) & \mathcal{S}_{1122} &= A(1+m)(1-\gamma+m) \\ \mathcal{S}_{1212} &= A(1+m^2+\gamma) & \mathcal{S}_{1112} &= \mathcal{S}_{2212} = \mathcal{S}_{1211} = \mathcal{S}_{1222} = 0 \end{aligned} \tag{61}$$

with $A = [8(1-\nu)]^{-1}$, $\gamma = 2(1-2\nu)$ and $m = (a_1 - a_2)/(a_1 + a_2)$. Then, substituting the above result into (58) and using therein the plane-strain versions $\boldsymbol{\mathcal{C}} = \bar{\kappa}\bar{\boldsymbol{\mathcal{J}}} + \mu\bar{\boldsymbol{\mathcal{K}}}$ and $\Delta\boldsymbol{\mathcal{C}} = \Delta\bar{\kappa}\boldsymbol{\mathcal{J}} + \Delta\mu\boldsymbol{\mathcal{K}}$ of the isotropic elastic constitutive relation (where $\bar{\kappa} := \kappa + \mu/3$ is the plane-strain bulk modulus, $\bar{\boldsymbol{\mathcal{J}}} := \boldsymbol{I} \otimes \boldsymbol{I}/2$ and $\bar{\boldsymbol{\mathcal{K}}} := \boldsymbol{\mathcal{I}} - \bar{\boldsymbol{\mathcal{J}}}$), exact algebraic formulae are obtained for the components of $\boldsymbol{\mathcal{A}}$, which have been checked to coincide with the corresponding result of **[43]** (Theorem 3.2), established using a different method.

5. Energy-based functionals. Another important class of functionals are those acting on the displacement gradient, or the linearized strain tensor, rather than the displacement. They include energy-like quantities such as the strain energy or energy-based error functionals.

To highlight issues specific to this kind of functional, let

$$E(\boldsymbol{\mathcal{C}}_a) = \mathbb{E}(\boldsymbol{u}_a) \qquad \text{with} \quad \mathbb{E}(\boldsymbol{w}) = \int_\Omega \Psi(\boldsymbol{\nabla w}) \, \mathrm{d}V \tag{62}$$

(where the density $\boldsymbol{X} \in \mathbb{R}^{3,3} \mapsto \Psi(\boldsymbol{X})$ is twice differentiable) and consider the first-order term arising from a pointwise Taylor expansion of $\Psi(\boldsymbol{\nabla u}_a)$ about $\boldsymbol{\nabla u}$:

$$E^1(\boldsymbol{\mathcal{C}}_a) := \mathbb{E}'(\boldsymbol{u}; \boldsymbol{v}_a) = \int_\Omega \Psi'(\boldsymbol{\nabla u}) : \boldsymbol{\nabla v}_a \, \mathrm{d}V$$

Defining an adjoint solution $\boldsymbol{q}$ by the weak formulation

$$\langle \boldsymbol{q}, \boldsymbol{w} \rangle_\Omega^{\mathcal{C}} = \mathbb{E}'(\boldsymbol{u}; \boldsymbol{w}) \qquad \forall \boldsymbol{w} \in W_0 \tag{63}$$

one then obtains (following the derivation (50) and invoking Lemma 2)

$$E^1(\boldsymbol{\mathcal{C}}_a) = \langle \boldsymbol{q}, \boldsymbol{v}_a \rangle_\Omega^{\mathcal{C}} = -\langle \boldsymbol{q}, \boldsymbol{u}_a \rangle_{B_a}^{\Delta\mathcal{C}} = O(a^3), \tag{64}$$

hence the contribution arising from the first-order Taylor expansion of $\Psi(\boldsymbol{\nabla u}_a)$ is again of order $O(a^3)$. However, (43) and (44) also imply that the second-order contribution from $\Psi(\boldsymbol{\nabla u}_a)$ yields

$$E^2(\boldsymbol{\mathcal{C}}_a) := \int_\Omega \boldsymbol{\nabla v}_a : \Psi''(\boldsymbol{\nabla u}) : \boldsymbol{\nabla v}_a \, \mathrm{d}V = O(a^3)$$

Since $E^1(\mathcal{C}_a)$ and $E^2(\mathcal{C}_a)$ are both of order $O(a^3)$ as $a \to 0$, the leading contribution of $E(\mathcal{C}_a) - E(\mathcal{C})$ as $a \to 0$ clearly does not coincide with that of $E^1(\mathcal{C}_a)$, unlike for the previously-considered class (16) of functionals. The derivation (64) does not yield the topological derivative of $E(\mathcal{C}_a)$, which also incorporates higher-order contributions from $\Psi(\boldsymbol{\nabla} \boldsymbol{u}_a)$ and must be established by means of a distinct treatment.

In the remainder of this section, the topological derivative is established for two energy-based functionals that depend quadratically on $\boldsymbol{\nabla} \boldsymbol{u}_a$. In addition to being of a physically natural and commonly encountered format, such functionals have *exact* expansions of the form $E(\mathcal{C}_a) = E(\mathcal{C}) + E^1(\mathcal{C}_a) + E^2(\mathcal{C}_a)$.

5.1. Two examples of energy-based functionals. The first kind of energy functional measures the error in strain energy between $\boldsymbol{u}_a$ and a given vector field $\boldsymbol{u}_0 \in H^1(\Omega;\mathbb{R}^3)$, and is defined by

$$E_1(\mathcal{C}_a) = \mathbb{E}_1(\boldsymbol{u}_a, \mathcal{C}_a) = \tfrac{1}{2}\langle \boldsymbol{u}_a - \boldsymbol{u}_0, \boldsymbol{u}_a - \boldsymbol{u}_0 \rangle_\Omega^{\mathcal{C}_a} \tag{65}$$

The particular case of the strain energy of $\boldsymbol{u}_a$ corresponds to setting $\boldsymbol{u}_0 = \boldsymbol{0}$ in (65).

The second kind of energy functional is the elastic counterpart of the functional used in **[10]** for electric impedance tomography. It is used for e.g. material or flaw identification from overdetermined boundary data. Let $\Gamma_{\mathrm{N}} = \Gamma_{\mathrm{o}} \cup \Gamma_{\mathrm{no}}$, assuming that a measurement $\boldsymbol{u}_{\mathrm{obs}}$ of the displacement induced in the solid by the excitation $(\boldsymbol{f}, \boldsymbol{g}, \bar{\boldsymbol{u}})$ defined in Sec. 1 is available on Γ_{o}. One can then define 'Neumann' and 'Dirichlet' displacement fields that differ only by their boundary data on Γ_{o}, on which either forces or displacements may be prescribed (the remaining data being as in Sec 1). The 'Neumann' and 'Dirichlet' fields coincide for perfect measurement $\boldsymbol{u}_{\mathrm{obs}}$ and a flawless solid with correctly known material characteristics, whereas a discrepancy between them reveals that the model for the reference solid is incorrect, e.g. due to the presence of a hidden defect. The 'Neumann' and 'Dirichlet' background fields $\boldsymbol{u}^{\mathrm{N}}$ and $\boldsymbol{u}^{\mathrm{D}}$ are defined by the following weak formulations:

$$\text{Find } \boldsymbol{u}^{\mathrm{N}} \in W^{\mathrm{N}}(\bar{\boldsymbol{u}}), \qquad \langle \boldsymbol{u}^{\mathrm{N}}, \boldsymbol{w} \rangle_\Omega^{\mathcal{C}} = F(\boldsymbol{w}), \qquad \forall \boldsymbol{w} \in W_0^{\mathrm{N}}. \tag{66a}$$

$$\text{Find } \boldsymbol{u}^{\mathrm{D}} \in W^{\mathrm{D}}(\bar{\boldsymbol{u}}), \qquad \langle \boldsymbol{u}^{\mathrm{D}}, \boldsymbol{w} \rangle_\Omega^{\mathcal{C}} = F(\boldsymbol{w}), \qquad \forall \boldsymbol{w} \in W_0^{\mathrm{D}}. \tag{66b}$$

having set $W^{\mathrm{D}}(\bar{\boldsymbol{u}}) = \big\{\boldsymbol{v} \in H^1(\Omega;\mathbb{R}^3),\ \boldsymbol{v} = \bar{\boldsymbol{u}} \text{ on } \Gamma_{\mathrm{D}},\ \boldsymbol{v} = \boldsymbol{u}_{\mathrm{obs}} \text{ on } \Gamma_{\mathrm{o}}\big\}$, $W_0^{\mathrm{D}} := W^{\mathrm{D}}(\boldsymbol{0})$ and $W^{\mathrm{N}}(\bar{\boldsymbol{u}}) = W(\bar{\boldsymbol{u}})$, $W_0^{\mathrm{N}} = W_0$ in terms of definition (6). Moreover, the 'Neumann' and 'Dirichlet' fields $\boldsymbol{u}_a^{\mathrm{N}}$ and $\boldsymbol{u}_a^{\mathrm{D}}$ for a small trial inhomogeneity B_a located at $\boldsymbol{z}$ are defined by the following weak formulations for the perturbations $\boldsymbol{v}_a^{\mathrm{N}} := \boldsymbol{u}_a^{\mathrm{N}} - \boldsymbol{u}^{\mathrm{N}}$ and $\boldsymbol{v}_a^{\mathrm{D}} := \boldsymbol{u}_a^{\mathrm{D}} - \boldsymbol{u}^{\mathrm{D}}$:

$$\text{Find } \boldsymbol{v}_a^{\mathrm{N}} \in W_0^{\mathrm{N}}, \qquad \langle \boldsymbol{v}_a^{\mathrm{N}}, \boldsymbol{w} \rangle_\Omega^{\mathcal{C}} + \langle \boldsymbol{v}_a^{\mathrm{N}}, \boldsymbol{w} \rangle_{B_a}^{\Delta\mathcal{C}} = -\langle \boldsymbol{u}^{\mathrm{N}}, \boldsymbol{w} \rangle_{B_a}^{\Delta\mathcal{C}}, \qquad \forall \boldsymbol{w} \in W_0^{\mathrm{N}}. \tag{67a}$$

$$\text{Find } \boldsymbol{v}_a^{\mathrm{D}} \in W_0^{\mathrm{D}}, \qquad \langle \boldsymbol{v}_a^{\mathrm{D}}, \boldsymbol{w} \rangle_\Omega^{\mathcal{C}} + \langle \boldsymbol{v}_a^{\mathrm{D}}, \boldsymbol{w} \rangle_{B_a}^{\Delta\mathcal{C}} = -\langle \boldsymbol{u}^{\mathrm{D}}, \boldsymbol{w} \rangle_{B_a}^{\Delta\mathcal{C}}, \qquad \forall \boldsymbol{w} \in W_0^{\mathrm{D}}. \tag{67b}$$

The energy functional $E_2(\mathcal{C}_a)$ is then defined so as to evaluate the 'Neumann'–'Dirichlet' discrepancy through the strain energy of the difference $\boldsymbol{u}_a^{\mathrm{N}} - \boldsymbol{u}_a^{\mathrm{D}}$ defined in terms of the perturbed material $\mathcal{C}_a$, i.e.:

$$E_2(\mathcal{C}_a) = \mathbb{E}_2(\boldsymbol{u}_a^{\mathrm{N}}, \boldsymbol{u}_a^{\mathrm{D}}, \mathcal{C}_a) = \tfrac{1}{2}\langle \boldsymbol{u}_a^{\mathrm{N}} - \boldsymbol{u}_a^{\mathrm{D}}, \boldsymbol{u}_a^{\mathrm{N}} - \boldsymbol{u}_a^{\mathrm{D}} \rangle_\Omega^{\mathcal{C}_a} \tag{68}$$

5.2. Topological derivative of functionals E_1, E_2.

Proposition 7. *The topological derivative of the energy functional $E_1(\mathcal{C}_a)$ is given by*

$$DE_1(\boldsymbol{z}) = \frac{|\mathcal{B}|}{2}\boldsymbol{\varepsilon}[\boldsymbol{u}_0](\boldsymbol{z}) : \Delta\mathcal{C} : \boldsymbol{\varepsilon}[\boldsymbol{u}_0](\boldsymbol{z}) - \frac{1}{2}\boldsymbol{\varepsilon}[\boldsymbol{u}](\boldsymbol{z}) : \boldsymbol{\mathcal{A}} : \boldsymbol{\varepsilon}[\boldsymbol{u} + 2\boldsymbol{q}](\boldsymbol{z}) \tag{69}$$

where the adjoint solution $\boldsymbol{q}$ is defined by the weak formulation

$$\textit{Find } \boldsymbol{q} \in W(\gamma_D(\boldsymbol{u}_0 - \boldsymbol{u})), \qquad \langle \boldsymbol{q}, \boldsymbol{w} \rangle_\Omega^{\mathcal{C}} = 0, \quad \forall \boldsymbol{w} \in W_0, \tag{70}$$

(with $\gamma_D(\boldsymbol{w})$ denoting the trace on Γ_D of $\boldsymbol{w} \in H^1(\Omega;\mathbb{R}^3)$).

The topological derivative of the energy functional $E_2(\mathcal{C}_a)$ is given by

$$DE_2(\boldsymbol{z}) = \frac{1}{2}\boldsymbol{\varepsilon}[\boldsymbol{u}^D](\boldsymbol{z}) : \boldsymbol{\mathcal{A}} : \boldsymbol{\varepsilon}[\boldsymbol{u}^D](\boldsymbol{z}) - \frac{1}{2}\boldsymbol{\varepsilon}[\boldsymbol{u}^N](\boldsymbol{z}) : \boldsymbol{\mathcal{A}} : \boldsymbol{\varepsilon}[\boldsymbol{u}^N](\boldsymbol{z}) \tag{71}$$

In both (69) and (71), $\boldsymbol{\mathcal{A}}$ denotes again the elastic moment tensor (19).

Proof. The functional $E_1(\boldsymbol{\mathcal{C}}_a)$ depends quadratically on $\boldsymbol{v}_a$. Expanding $E_1(\boldsymbol{\mathcal{C}}_a)$ into terms of order 0, 1 and 2 in $\boldsymbol{v}_a$, one obtains the following, exact, expression:

$$2E_1(\boldsymbol{\mathcal{C}}_a) - 2E_1(\boldsymbol{\mathcal{C}}) = \langle \boldsymbol{u}-\boldsymbol{u}_0, \boldsymbol{u}-\boldsymbol{u}_0\rangle_{B_a}^{\Delta\mathcal{C}} + 2\langle \boldsymbol{u}-\boldsymbol{u}_0, \boldsymbol{v}_a\rangle_{\Omega}^{\mathcal{C}_a} + \langle \boldsymbol{v}_a, \boldsymbol{v}_a\rangle_{\Omega}^{\mathcal{C}_a} \tag{72}$$

The definition (70) of the adjoint field $\boldsymbol{q}$ implies that $\boldsymbol{q}+\boldsymbol{u}-\boldsymbol{u}_0 \in W_0$. Hence, one may set $\boldsymbol{w} = \boldsymbol{q}+\boldsymbol{u}-\boldsymbol{u}_0$ in (12), to obtain after some manipulation:

$$\langle \boldsymbol{u}-\boldsymbol{u}_0, \boldsymbol{v}_a\rangle_{\Omega}^{\mathcal{C}} = \langle \boldsymbol{q}+\boldsymbol{u}-\boldsymbol{u}_0, \boldsymbol{v}_a\rangle_{\Omega}^{\mathcal{C}} = -\langle \boldsymbol{q}+\boldsymbol{u}-\boldsymbol{u}_0, \boldsymbol{u}_a\rangle_{B_a}^{\Delta\mathcal{C}}$$

(where the first equality exploits (70) with $\boldsymbol{w} = \boldsymbol{v}_a \in W_0$)), and thus

$$\langle \boldsymbol{u}-\boldsymbol{u}_0, \boldsymbol{v}_a\rangle_{\Omega}^{\mathcal{C}_a} = \langle \boldsymbol{u}-\boldsymbol{u}_0, \boldsymbol{v}_a\rangle_{B_a}^{\Delta\mathcal{C}} - \langle \boldsymbol{q}+\boldsymbol{u}-\boldsymbol{u}_0, \boldsymbol{u}_a\rangle_{B_a}^{\Delta\mathcal{C}} = -\langle \boldsymbol{u}-\boldsymbol{u}_0, \boldsymbol{u}\rangle_{B_a}^{\Delta\mathcal{C}} - \langle \boldsymbol{q}, \boldsymbol{u}_a\rangle_{B_a}^{\Delta\mathcal{C}}$$

Next, weak formulation (12) with $\boldsymbol{w} = \boldsymbol{v}_a$ yields

$$\langle \boldsymbol{v}_a, \boldsymbol{v}_a\rangle_{\Omega}^{\mathcal{C}_a} = -\langle \boldsymbol{u}, \boldsymbol{v}_a\rangle_{B_a}^{\Delta\mathcal{C}}$$

Finally, inserting the last two equalities into (72) and rearranging terms, one finds

$$\begin{aligned} 2E_1(\boldsymbol{\mathcal{C}}_a) - 2E_1(\boldsymbol{\mathcal{C}}) &= -\langle \boldsymbol{u}-\boldsymbol{u}_0, \boldsymbol{u}+\boldsymbol{u}_0\rangle_{B_a}^{\Delta\mathcal{C}} - 2\langle \boldsymbol{q}, \boldsymbol{u}_a\rangle_{B_a}^{\Delta\mathcal{C}} - \langle \boldsymbol{u}, \boldsymbol{v}_a\rangle_{B_a}^{\Delta\mathcal{C}} \\ &= \langle \boldsymbol{u}_0, \boldsymbol{u}_0\rangle_{B_a}^{\Delta\mathcal{C}} - \langle \boldsymbol{u}+2\boldsymbol{q}, \boldsymbol{u}_a\rangle_{B_a}^{\Delta\mathcal{C}}, \end{aligned}$$

with the desired result (69) following by applying Lemma (51) for the last term of the right-hand side.

The functional $E_2(\boldsymbol{\mathcal{C}}_a)$ depending quadratically on $\boldsymbol{v}_a^{\mathrm{D}}, \boldsymbol{v}_a^{\mathrm{N}}$, one obtains the alternative expression:

$$\begin{aligned} 2E_2(\boldsymbol{\mathcal{C}}_a) - 2E_2(\boldsymbol{\mathcal{C}}) &= \langle \boldsymbol{u}^{\mathrm{N}}-\boldsymbol{u}^{\mathrm{D}}, \boldsymbol{u}^{\mathrm{N}}-\boldsymbol{u}^{\mathrm{D}}\rangle_{B_a}^{\Delta\mathcal{C}} \\ &\quad + 2\langle \boldsymbol{u}^{\mathrm{N}}-\boldsymbol{u}^{\mathrm{D}}, \boldsymbol{v}_a^{\mathrm{N}}-\boldsymbol{v}_a^{\mathrm{D}}\rangle_{\Omega}^{\mathcal{C}_a} + \langle \boldsymbol{v}_a^{\mathrm{N}}-\boldsymbol{v}_a^{\mathrm{D}}, \boldsymbol{v}_a^{\mathrm{N}}-\boldsymbol{v}_a^{\mathrm{D}}\rangle_{\Omega}^{\mathcal{C}_a} \end{aligned} \tag{73}$$

Now, using weak formulation (12) with $(\boldsymbol{v}_a, \boldsymbol{w})$ replaced in succession by $(\boldsymbol{v}_a^{\mathrm{N}}, \boldsymbol{v}_a^{\mathrm{N}}) \in W_0^{\mathrm{N}} \times W_0^{\mathrm{N}}$, $(\boldsymbol{v}_a^{\mathrm{D}}, \boldsymbol{v}_a^{\mathrm{D}}) \in W_0^{\mathrm{D}} \times W_0^{\mathrm{D}}$ and $(\boldsymbol{v}_a^{\mathrm{N}}, \boldsymbol{v}_a^{\mathrm{D}}) \in W_0^{\mathrm{N}} \times W_0^{\mathrm{N}}$ (noting for the last case that $\boldsymbol{v}_a^{\mathrm{D}} \in W_0^{\mathrm{D}} \subset W_0^{\mathrm{N}}$), one obtains the identities

$$\langle \boldsymbol{v}_a^{\mathrm{N}}, \boldsymbol{v}_a^{\mathrm{N}}\rangle_{\Omega}^{\mathcal{C}_a} = -\langle \boldsymbol{u}^{\mathrm{N}}, \boldsymbol{v}_a^{\mathrm{N}}\rangle_{B_a}^{\Delta\mathcal{C}}, \qquad \langle \boldsymbol{v}_a^{\mathrm{D}}, \boldsymbol{v}_a^{\mathrm{D}}\rangle_{\Omega}^{\mathcal{C}_a} = -\langle \boldsymbol{u}^{\mathrm{D}}, \boldsymbol{v}_a^{\mathrm{D}}\rangle_{B_a}^{\Delta\mathcal{C}}, \qquad \langle \boldsymbol{v}_a^{\mathrm{N}}, \boldsymbol{v}_a^{\mathrm{D}}\rangle_{\Omega}^{\mathcal{C}_a} = -\langle \boldsymbol{u}^{\mathrm{N}}, \boldsymbol{v}_a^{\mathrm{D}}\rangle_{B_a}^{\Delta\mathcal{C}},$$

and hence

$$\langle \boldsymbol{v}_a^{\mathrm{N}}-\boldsymbol{v}_a^{\mathrm{D}}, \boldsymbol{v}_a^{\mathrm{N}}-\boldsymbol{v}_a^{\mathrm{D}}\rangle_{\Omega}^{\mathcal{C}_a} = -\langle \boldsymbol{u}^{\mathrm{N}}, \boldsymbol{v}_a^{\mathrm{N}}\rangle_{B_a}^{\Delta\mathcal{C}} - \langle \boldsymbol{u}^{\mathrm{D}}-2\boldsymbol{u}^{\mathrm{N}}, \boldsymbol{v}_a^{\mathrm{D}}\rangle_{B_a}^{\Delta\mathcal{C}} \tag{74}$$

Next, using again weak formulation (12), this time with $(\boldsymbol{v}_a, \boldsymbol{w})$ replaced by $(\boldsymbol{v}_a^{\mathrm{N}}, \boldsymbol{u}^{\mathrm{N}}-\boldsymbol{u}^{\mathrm{D}}) \in W_0^{\mathrm{N}} \times W_0^{\mathrm{N}}$, one has

$$\langle \boldsymbol{u}^{\mathrm{N}}-\boldsymbol{u}^{\mathrm{D}}, \boldsymbol{v}_a^{\mathrm{N}}\rangle_{\Omega}^{\mathcal{C}_a} = -\langle \boldsymbol{u}^{\mathrm{N}}, \boldsymbol{u}^{\mathrm{N}}-\boldsymbol{u}^{\mathrm{D}}\rangle_{B_a}^{\Delta\mathcal{C}}$$

while invoking weak formulations (66a) and (66b) with $\boldsymbol{w} = \boldsymbol{v}_a^{\mathrm{D}} \in W_0^{\mathrm{D}} \subset W_0^{\mathrm{N}}$ yields

$$\langle \boldsymbol{u}^{\mathrm{N}}-\boldsymbol{u}^{\mathrm{D}}, \boldsymbol{v}_a^{\mathrm{D}}\rangle_{\Omega}^{\mathcal{C}} = 0$$

Combining the last two identities, one obtains

$$\langle \boldsymbol{u}^{\mathrm{N}}-\boldsymbol{u}^{\mathrm{D}}, \boldsymbol{v}_a^{\mathrm{N}}-\boldsymbol{v}_a^{\mathrm{D}}\rangle_{\Omega}^{\mathcal{C}_a} = -\langle \boldsymbol{u}^{\mathrm{N}}-\boldsymbol{u}^{\mathrm{D}}, \boldsymbol{v}_a^{\mathrm{D}}\rangle_{B_a}^{\Delta\mathcal{C}} - \langle \boldsymbol{u}^{\mathrm{N}}, \boldsymbol{u}^{\mathrm{N}}-\boldsymbol{u}^{\mathrm{D}}\rangle_{B_a}^{\Delta\mathcal{C}} \tag{75}$$

Substituting (74) and (75) into (73) and rearranging terms yields

$$\begin{aligned} 2E_2(\boldsymbol{\mathcal{C}}_a) - 2E_2(\boldsymbol{\mathcal{C}}) &= \langle \boldsymbol{u}^{\mathrm{D}}, \boldsymbol{u}^{\mathrm{D}}\rangle_{B_a}^{\Delta\mathcal{C}} - \langle \boldsymbol{u}^{\mathrm{N}}, \boldsymbol{u}^{\mathrm{N}}\rangle_{B_a}^{\Delta\mathcal{C}} + \langle \boldsymbol{u}^{\mathrm{D}}, \boldsymbol{v}_a^{\mathrm{D}}\rangle_{B_a}^{\Delta\mathcal{C}} - \langle \boldsymbol{u}^{\mathrm{N}}, \boldsymbol{v}_a^{\mathrm{N}}\rangle_{B_a}^{\Delta\mathcal{C}} \\ &= \langle \boldsymbol{u}^{\mathrm{D}}, \boldsymbol{u}_a^{\mathrm{D}}\rangle_{B_a}^{\Delta\mathcal{C}} - \langle \boldsymbol{u}^{\mathrm{N}}, \boldsymbol{u}_a^{\mathrm{N}}\rangle_{B_a}^{\Delta\mathcal{C}}. \end{aligned}$$

The sought result (71) finally stems from applying (51) to each term of the right-hand side in the above equality. □

6. Numerical results. This section presents three kinds of numerical results. First, in view of the essential role of the EMT $\boldsymbol{\mathcal{A}}$ in the evaluation of DJ, its computation is examined in Sec. 6.1 for ellipsoidal (or spherical) inhomogeneities, corresponding to the most often used form of topological derivative. In

this case, (58) shows that an accurate evaluation of $\boldsymbol{\mathcal{A}}$ mainly hinges on that of $\boldsymbol{\mathcal{S}}$, which is thus the main focus of Sec. 6.1. Then, a numerical validation of expression (53) for DJ, performed in 2D conditions by comparing $J(\mathcal{C}_a)$ evaluated either numerically or using expansion (18), is presented in Sec. 6.2. Finally, Sec. 6.3 illustrates flaw identification using the topological derivative of the energy functional E_1.

6.1. Numerical evaluation of the EMT for ellipsoidal inhomogeneities. Considering an ellipsoidal inhomogeneity shape $\mathcal{B}$, the computation of $\boldsymbol{\mathcal{A}}$ using (58) is straightforward once $\boldsymbol{\mathcal{S}}$ is known. Evaluating the latter usually requires a numerical quadrature of integral (56). A set of high-accuracy quadrature rules specially designed for integrals over Σ, proposed in [**44**], are used here for this purpose. Each such rule is based on a set of N_L points $\hat{\boldsymbol{\eta}}_q \in \Sigma$ and weights w_q, determined so as to integrate exactly spherical harmonics of order up to L (they are freely available, as a Matlab file `getLebedevSphere.m`, from e.g. `www.mathworks.com`). Formula (56) then becomes

$$\mathcal{S}_{ijk\ell} = \frac{1}{8\pi}\mathcal{C}_{mnk\ell}\sum_{q=1}^{N_L} w_q\big[\eta_{q,j}N_{im}(\boldsymbol{\eta}_q) + \eta_{q,i}N_{jm}(\boldsymbol{\eta}_q)\big]\eta_{q,n}(\theta) + \epsilon(N_L) \tag{76}$$

(where $\epsilon(N_L)$ denotes the quadrature error). In this section, the accuracy of the numerical computation of $\boldsymbol{\mathcal{S}}$ is quantified in terms of the relative L^∞ discrepancy between $\boldsymbol{\mathcal{S}}$ and a reference value $\boldsymbol{\mathcal{S}}^{\mathrm{ref}}$, denoted $e(\boldsymbol{\mathcal{S}})$ and defined by

$$e(\boldsymbol{\mathcal{S}}) := \frac{|\boldsymbol{\mathcal{S}} - \boldsymbol{\mathcal{S}}^{\mathrm{ref}}|_\infty}{|\boldsymbol{\mathcal{S}}^{\mathrm{ref}}|_\infty} = \frac{\max_{i,j,k,\ell}|\mathcal{S}_{ijk\ell} - \mathcal{S}^{\mathrm{ref}}_{ijk\ell}|}{\max_{i,j,k,\ell}|\mathcal{S}^{\mathrm{ref}}_{ijk\ell}|}, \tag{77}$$

First, three cases with available analytical exact solutions $\boldsymbol{\mathcal{S}}^{\mathrm{ref}}$ are considered, namely (a) a spherical inclusion ($a_1 = a_2 = a_3$), (b) a penny-shaped thin inclusion ($a_1 = a_2, a_3 \to 0$) and (c) a cylindrical inclusion with elliptical cross-section ($a_3 \to \infty$). An isotropic background material with a Poisson ratio $\nu = 0.3$ is assumed for all three cases. Numerical quadrature for cases (b) and (c) used $a_3 = 10^{-40}$ and $a_3 = 10^{40}$, respectively. In cases (a) and (b), (76) achieves an exact evaluation (within double-precision accuracy) with $N_5 = 14$ and $N_3 = 6$ quadrature points, respectively. Case (c) corresponds to an elliptical inclusion under two-dimensional plane-strain conditions, with the exact solution $\boldsymbol{\mathcal{S}}^{\mathrm{ref}}$ given by (61), but the numerical quadrature was still done using the three-dimensional formula (76), treating the inclusion as an extremely elongated ellipsoid ($a_3 = 10^{40}$) so as to test the numerical quadrature under more severe conditions. Relative errors $e(\boldsymbol{\mathcal{S}})$ achieved for various values of N_L and the aspect ratio a_2/a_1 of the cross-section are shown in Fig. 1. Clearly, due to the very high aspect ratio a_3/a_1 used, sufficient accuracy (say $e(\boldsymbol{\mathcal{S}}) \le 10^{-2}$) requires hundreds to thousands of quadrature points depending on the aspect ratio a_2/a_1.

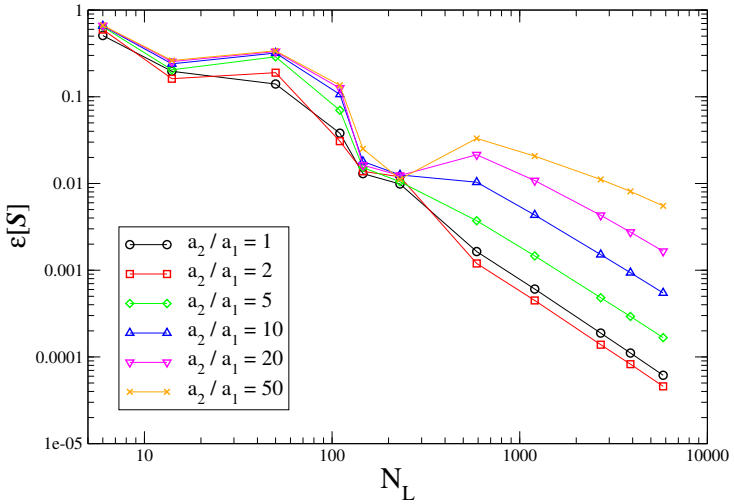

FIGURE 1. Cylindrical inclusion with elliptical cross-section: relative error $e(\boldsymbol{\mathcal{S}})$ as a function of quadrature order N_L for various values of aspect ratio a_2/a_1.

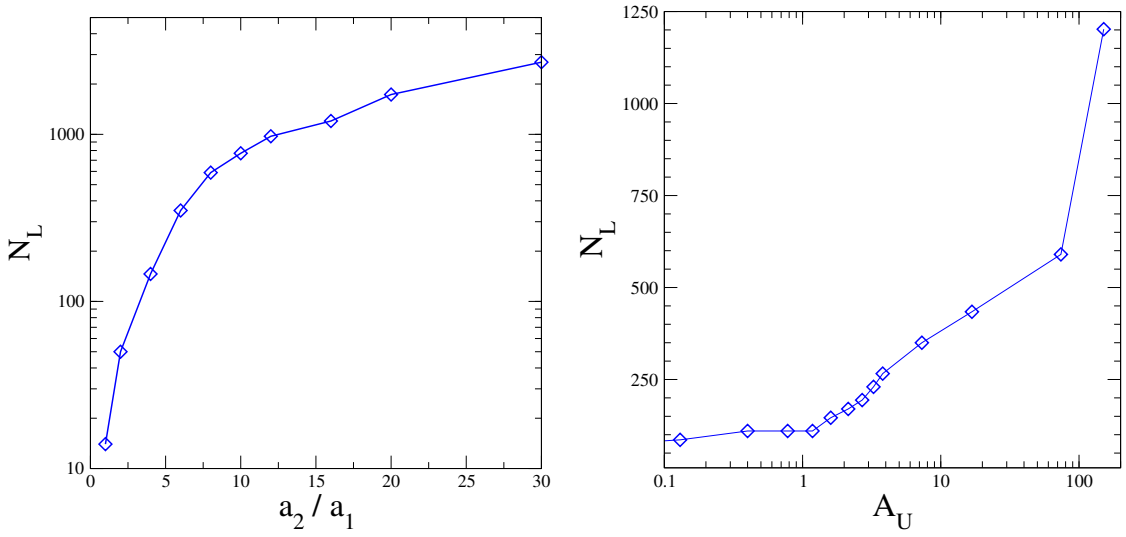

FIGURE 2. Quadrature order N_L needed to achieve target accuracy $e(\boldsymbol{\mathcal{S}}) = 10^{-5}$ for (a) isotropic background material and varying values of aspect ratio a_2/a_1 or (b) varying values of anisotropy index A_{U} of background material.

Next, the influence of either geometrical or material distortion on the quadrature order N_L required to achieve a fixed target accuracy $e(\boldsymbol{\mathcal{S}}) = 10^{-5}$ in (76) is investigated. In Fig. 2a, an ellipsoidal inclusion with semiaxes (a_1, a_2, a_1) in an isotropic background material is considered, with the aspect ratio a_2/a_1 varying over the range $[1, 30]$, while Fig. 2b corresponds to the case of a spherical inclusion in various anisotropic material, with the anisotropy index A_{U} **[45]** varying between 0 (isotropic) to about 150 (highly anisotropic). The definition and evaluation methodology of A_{U} are recalled for completeness in Appendix D. Clearly, suitable values of the quadrature order N_L are strongly influenced by both geometrical and material distortion. The latter effect is relevant in e.g. combined topology/material structural optimization, where the ability to accurately compute $DJ(\boldsymbol{z})$ for arbitrary trial materials spanning wide ranges of anisotropy is important.

6.2. Numerical assessment of the topological derivative. In this section, a simple cantilever structure featuring an anisotropic elliptic inhomogeneity B_a is considered, under plane-strain two-dimensional conditions (Fig. 3). The structure is clamped along its left side and loaded on its right side by $\boldsymbol{g} = (0, -1)$. No body forces are applied ($\boldsymbol{f} = 0$), and the remaining part of the boundary is traction-free. Two cases are considered for the constitutive properties: (a) a fully isotropic case with

$$\boldsymbol{\mathcal{C}} = \begin{pmatrix} 1.34 & 0.57 & 0. \\ 0.57 & 1.34 & 0. \\ 0. & 0. & 0.38 \end{pmatrix}, \qquad \boldsymbol{\mathcal{C}}^\star = 10^{-9}\boldsymbol{\mathcal{C}}$$

(using the Voigt matrix notation, which reduces to 3×3 matrices for the plane-strain case), i.e. with a very soft inhomogeneity close to a void, and (b) a fully anisotropic case with

$$\boldsymbol{\mathcal{C}} = \begin{pmatrix} 1. & 0.5 & 0. \\ 0.5 & 2. & 0. \\ 0. & 0. & 0.04 \end{pmatrix}, \qquad \boldsymbol{\mathcal{C}}^\star = \begin{pmatrix} 3. & 0.4 & 0. \\ 0.4 & 1.5 & 0. \\ 0. & 0. & 0.03 \end{pmatrix}$$

A specific objective function was considered, namely the potential energy

$$J(\boldsymbol{\mathcal{C}}_a) = \mathbb{E}_{\mathrm{pot}}(\boldsymbol{u}_a) := -\frac{1}{2}\int_{\Gamma_{\mathrm{N}}} \boldsymbol{u}_a \cdot \boldsymbol{g}\, \mathrm{d}s = -\frac{1}{2}\int_{\Gamma_{\mathrm{N}}} u_{a,2}\, \mathrm{d}s,$$

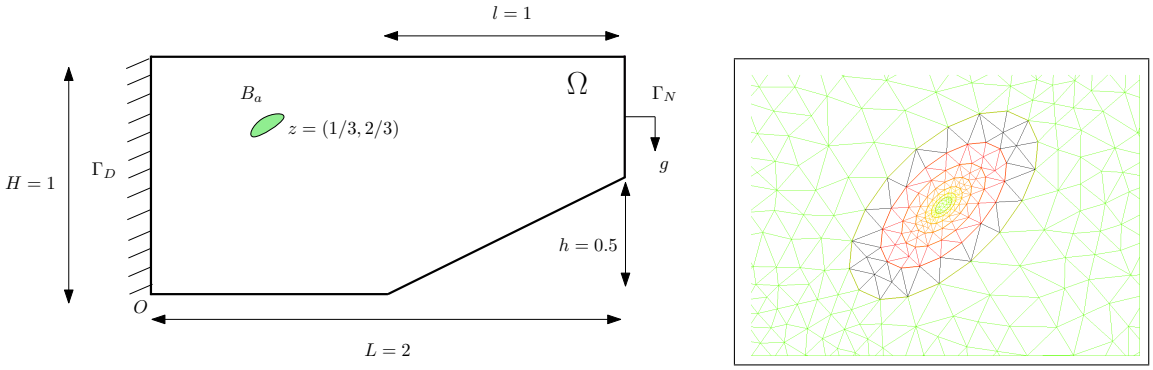

FIGURE 3. 2D Test case and the nested mesh structure of the inhomogeneities.

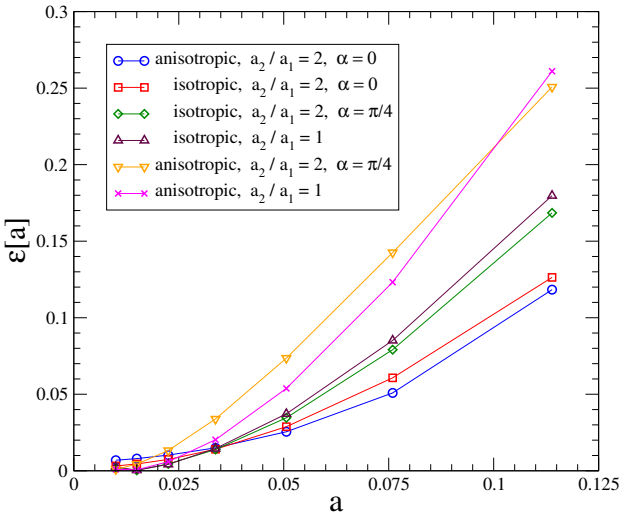

FIGURE 4. 2D Test case with nested inhomogeneities

whose topological derivative is given by (54). Finite element analyses for cases (a) and (b) with various (small) values of a were made using FreeFem++ **[46]**, while the computation of $DJ(\boldsymbol{z})$ relied on a Gauss-Legendre quadrature formula for the numerical evaluation of $\boldsymbol{\mathcal{S}}$ by means of (60).

The discrepancy $e(a)$ between $J(\mathcal{C}_a)$ evaluated either numerically or using expansion (18), defined by

$$e(a) := \frac{|\Delta J - a^2 DJ(\boldsymbol{z})|}{|a^2 DJ(\boldsymbol{z})|}, \qquad \text{with } \Delta J := J(\mathcal{C}_a) - J(\mathcal{C})$$

is plotted against a in Fig. 4, for an elliptic inhomogeneity with aspect ratio $a_1/a_2 = 1$ (disk) or 2 and (in the latter case) orientations $\alpha = 0$ or $\pi/4$. A numerical test of correctness of the evaluation of $DJ(\boldsymbol{z})$ then consists in checking that $e(a) = o(a)$ for small a. This desired trend is clearly visible for all considered cases in Fig. 4. The results there moreover suggest that $e(a) = O(a^2)$, even though one would *a priori* have expected a linear behavior. This empirical remark is consistent with higher-order topological expansions obtained in other situations **[47]** where for 2D problems the $O(a^3)$ contribution to the objective function expansion is found to vanish whenever the shape $\mathcal{B}$ has central symmetry, which is the case of an elliptic inhomogeneity.

Remark 12. *This asymptotic validation is here limited to the 2D case because accurate numerical results require a very fine mesh of the inhomogeneity and its vicinity.*

6.3. Flaw identification using an energy cost functional. To illustrate the usefulness of the topological derivative of energy-based cost functionals, the detection of three circular anisotropic inhomogeneities $B_k = B_a(\boldsymbol{z}_k)$ $(k = 1, 2, 3)$ having the same radius a and embedded in an anisotropic reference material is considered, again under two-dimensional plane-strain conditions (with geometry and background elastic properties $\boldsymbol{\mathcal{C}}$ as shown in Fig. 5). B_1 and B_3 are softer than the background ($\boldsymbol{\mathcal{C}}^\star = 0.5\boldsymbol{\mathcal{C}}$), while B_2 is harder ($\boldsymbol{\mathcal{C}}^\star = 2\boldsymbol{\mathcal{C}}$). The solid is clamped on its bottom and lateral sides, while a uniform normal pressure $g = 1$ is applied on its top side. The displacement response $\boldsymbol{u}_0$ of the flawed solid is computed using finite elements. The identification problem then consists of identifying the inclusions knowing the kinematic response $\boldsymbol{u}_0$, which may in practice be available from full-field measurement techniques such as digital image correlation. Here, the identification problem may be formulated as minimizing the functional E_1 defined by (65). Figure 6 shows the topological derivative $DE_1(\boldsymbol{z})$ (more precisely, the normalized and thresholded quantity $\boldsymbol{z} \mapsto \mathrm{Min}\big(DE_1(\boldsymbol{z}), 0\big)/\big[-\mathrm{Min}\big(DE_1(\boldsymbol{z})\big)\big]$), where the EMT is defined using either $\boldsymbol{\mathcal{C}}^\star = 0.5\boldsymbol{\mathcal{C}}$ or $\boldsymbol{\mathcal{C}}^\star = 2\boldsymbol{\mathcal{C}}$. According to the choice of EMT, the topological derivative field $DE_1(\boldsymbol{z})$ is seen to reveal correctly, through locations at which $DE_1(\boldsymbol{z})$ is most negative, the locations of the softer and stiffer flaws. This is consistent with similar findings made in **[28]** for the elastodynamic case and using least-squares output cost functionals. Similar results have been obtained on this example for cases where $\boldsymbol{\mathcal{C}}^\star$ is not proportional to $\boldsymbol{\mathcal{C}}$.

Appendix A. Proof of Proposition 3. From definition (19), for any $\boldsymbol{E} \in \mathbb{R}^{3,3}$, one has $\boldsymbol{E}:\boldsymbol{\mathcal{A}}:\boldsymbol{E} = |\mathcal{B}|\boldsymbol{E}:\Delta\boldsymbol{\mathcal{C}}:\boldsymbol{E} + \langle\boldsymbol{\varphi}[\boldsymbol{E}], \boldsymbol{v}_{\mathcal{B}}[\boldsymbol{E}]\rangle_{\mathcal{B}}^{\Delta\mathcal{C}}$. This proof now exploits two different reformulations of $\boldsymbol{E}:\boldsymbol{\mathcal{A}}:\boldsymbol{E}$. For a first reformulation, setting $\boldsymbol{w} = \boldsymbol{v}_{\mathcal{B}}$ in (15), one has $\langle\boldsymbol{\varphi}[\boldsymbol{E}], \boldsymbol{v}_{\mathcal{B}}[\boldsymbol{E}]\rangle_{\mathcal{B}}^{\Delta\mathcal{C}} = -\langle\boldsymbol{v}_{\mathcal{B}}[\boldsymbol{E}], \boldsymbol{v}_{\mathcal{B}}[\boldsymbol{E}]\rangle_{\mathcal{B}}^{\mathcal{C}_{\mathcal{B}}}$, and hence

$$\boldsymbol{E}:\boldsymbol{\mathcal{A}}:\boldsymbol{E} = |\mathcal{B}|\boldsymbol{E}:\Delta\boldsymbol{\mathcal{C}}:\boldsymbol{E} - \langle\boldsymbol{v}_{\mathcal{B}}[\boldsymbol{E}], \boldsymbol{v}_{\mathcal{B}}[\boldsymbol{E}]\rangle_{\mathcal{B}}^{\mathcal{C}_{\mathcal{B}}}. \tag{A.1}$$

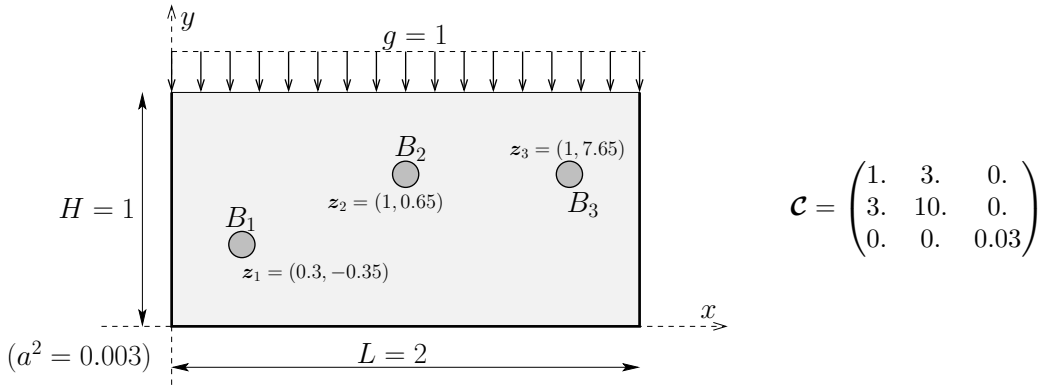

FIGURE 5. Flaw identification using an energy cost functional: setting and notations.

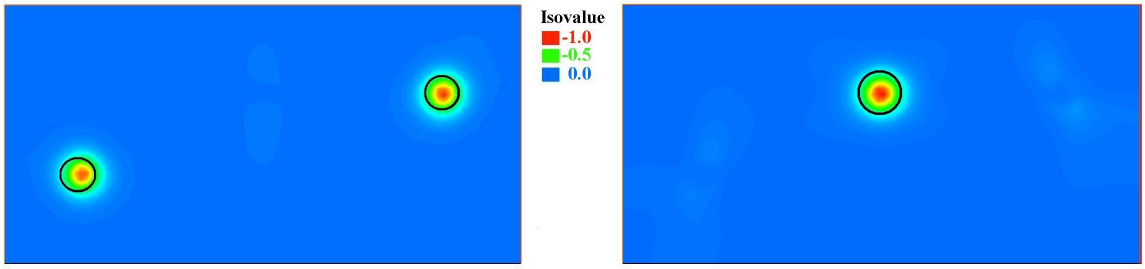

FIGURE 6. Flaw identification using an energy cost functional: topological derivative $DE_1(\boldsymbol{z})$.

For a second reformulation of $\boldsymbol{E}:\boldsymbol{\mathcal{A}}:\boldsymbol{E}$, let $\boldsymbol{Z}:=\boldsymbol{\mathcal{C}}^{\star-1}:\Delta\boldsymbol{\mathcal{C}}:\boldsymbol{E}\in\mathbb{R}^{3,3}_{\rm sym}$, so that $\langle\boldsymbol{\varphi}[\boldsymbol{Z}],\boldsymbol{w}\rangle_{\mathcal{B}}^{\mathcal{C}_\mathcal{B}}=\langle\boldsymbol{\varphi}[\boldsymbol{E}],\boldsymbol{w}\rangle_{\mathcal{B}}^{\Delta\mathcal{C}}$ holds for any $\boldsymbol{w}\in H^1(\mathcal{B};\mathbb{R}^3)$, and define $\hat{\boldsymbol{v}}_\mathcal{B}[\boldsymbol{E}]:=\boldsymbol{v}_\mathcal{B}[\boldsymbol{E}]+\boldsymbol{\varphi}[\boldsymbol{Z}]$ in $\mathcal{B}$. Then:

$$\begin{aligned}\langle\boldsymbol{\varphi}[\boldsymbol{E}],\boldsymbol{v}_\mathcal{B}[\boldsymbol{E}]\rangle_{\mathcal{B}}^{\Delta\mathcal{C}}&=\langle\boldsymbol{\varphi}[\boldsymbol{Z}],\boldsymbol{v}_\mathcal{B}[\boldsymbol{E}]\rangle_{\mathcal{B}}^{\mathcal{C}_\mathcal{B}}\\&=\langle\hat{\boldsymbol{v}}_\mathcal{B}[\boldsymbol{E}]-\boldsymbol{v}_\mathcal{B}[\boldsymbol{E}],\boldsymbol{v}_\mathcal{B}[\boldsymbol{E}]\rangle_{\mathcal{B}}^{\mathcal{C}_\mathcal{B}}\\&=\langle\hat{\boldsymbol{v}}_\mathcal{B}[\boldsymbol{E}],\hat{\boldsymbol{v}}_\mathcal{B}[\boldsymbol{E}]\rangle_{\mathcal{B}}^{\mathcal{C}_\mathcal{B}}-\langle\hat{\boldsymbol{v}}_\mathcal{B}[\boldsymbol{E}],\boldsymbol{\varphi}[\boldsymbol{Z}]\rangle_{\mathcal{B}}^{\mathcal{C}_\mathcal{B}}-\langle\boldsymbol{v}_\mathcal{B}[\boldsymbol{E}],\boldsymbol{v}_\mathcal{B}[\boldsymbol{E}]\rangle_{\mathcal{B}}^{\mathcal{C}_\mathcal{B}}\end{aligned}\tag{A.2}$$

Now, setting again $\boldsymbol{w}=\boldsymbol{v}_\mathcal{B}$ in (15), one obtains

$$\langle\boldsymbol{v}_\mathcal{B}[\boldsymbol{E}],\boldsymbol{v}_\mathcal{B}[\boldsymbol{E}]\rangle_{\mathcal{B}}^{\mathcal{C}_\mathcal{B}}=-\langle\boldsymbol{v}_\mathcal{B}[\boldsymbol{E}],\boldsymbol{v}_\mathcal{B}[\boldsymbol{E}]\rangle_{\mathbb{R}^3\setminus\mathcal{B}}^{\mathcal{C}_\mathcal{B}}-\langle\boldsymbol{\varphi}[\boldsymbol{E}],\boldsymbol{v}_\mathcal{B}[\boldsymbol{E}]\rangle_{\mathcal{B}}^{\Delta\mathcal{C}}.$$

Inserting this identity in the last equality of (A.2), using $\langle\hat{\boldsymbol{v}}_\mathcal{B}[\boldsymbol{E}],\boldsymbol{\varphi}[\boldsymbol{Z}]\rangle_{\mathcal{B}}^{\mathcal{C}_\mathcal{B}}=\langle\hat{\boldsymbol{v}}_\mathcal{B}[\boldsymbol{E}],\boldsymbol{\varphi}[\boldsymbol{E}]\rangle_{\mathcal{B}}^{\Delta\mathcal{C}}$ and noting that $|\mathcal{B}|\boldsymbol{E}:\Delta\boldsymbol{\mathcal{C}}:\boldsymbol{E}=\langle\boldsymbol{\varphi}[\boldsymbol{E}],\boldsymbol{\varphi}[\boldsymbol{E}]\rangle_{\mathcal{B}}^{\Delta\mathcal{C}}$, the sought reformulation is finally:

$$\boldsymbol{E}:\boldsymbol{\mathcal{A}}:\boldsymbol{E}=\langle\hat{\boldsymbol{v}}_\mathcal{B}[\boldsymbol{E}],\hat{\boldsymbol{v}}_\mathcal{B}[\boldsymbol{E}]\rangle_{\mathcal{B}}^{\mathcal{C}_\mathcal{B}}+\langle\boldsymbol{v}_\mathcal{B}[\boldsymbol{E}],\boldsymbol{v}_\mathcal{B}[\boldsymbol{E}]\rangle_{\mathbb{R}^3\setminus\mathcal{B}}^{\mathcal{C}_\mathcal{B}}+\langle\boldsymbol{\varphi}[\boldsymbol{E}],\boldsymbol{\varphi}[\boldsymbol{E}-\boldsymbol{Z}]\rangle_{\mathcal{B}}^{\mathcal{C}_\mathcal{B}}\tag{A.3}$$

Let now $\boldsymbol{E}$ be an eigentensor associated vith eigenvalue Λ for problem (26).

First, (26) then implies $\boldsymbol{E}:\Delta\boldsymbol{\mathcal{C}}:\boldsymbol{E}=(\Lambda-1)\boldsymbol{E}:\boldsymbol{\mathcal{C}}:\boldsymbol{E}$; moreover, the last term in the right-hand side of (A.1) is non-positive. Therefore, $\boldsymbol{E}:\boldsymbol{\mathcal{A}}:\boldsymbol{E}<0$ for any eigenvalue $\Lambda<1$.

Then, to exploit the second reformulation (A.3), a simple derivation yields

$$\langle\boldsymbol{\varphi}[\boldsymbol{E}],\boldsymbol{\varphi}[\boldsymbol{E}-\boldsymbol{Z}]\rangle_{\mathcal{B}}^{\mathcal{C}_\mathcal{B}}=|\mathcal{B}|\boldsymbol{E}:\Delta\boldsymbol{\mathcal{C}}:\boldsymbol{\mathcal{C}}^{\star-1}:\boldsymbol{\mathcal{C}}:\boldsymbol{E}=|\mathcal{B}|(\Lambda-1)\boldsymbol{E}:\boldsymbol{\mathcal{C}}:\boldsymbol{\mathcal{C}}^{\star-1}:\boldsymbol{\mathcal{C}}:\boldsymbol{E}.$$

The above quantity is positive for $\Lambda>1$ while the other terms in the right-hand side of (A.3) are non-negative. Therefore, $\boldsymbol{E}:\boldsymbol{\mathcal{A}}:\boldsymbol{E}>0$ for any eigenvalue $\Lambda>1$.

Finally, the proof of Proposition 3 is completed by noting that if $\Lambda=1$, an eigenvector $\boldsymbol{E}$ verifies $\Delta\boldsymbol{\mathcal{C}}:\boldsymbol{E}=\boldsymbol{0}$. This implies that $\boldsymbol{E}:\boldsymbol{\mathcal{A}}:\boldsymbol{E}=|\mathcal{B}|\boldsymbol{E}:\Delta\boldsymbol{\mathcal{C}}:\boldsymbol{E}+\langle\boldsymbol{\varphi}[\boldsymbol{E}],\boldsymbol{v}_\mathcal{B}[\boldsymbol{E}]\rangle_{\mathcal{B}}^{\Delta\mathcal{C}}=0$.

Appendix B. Proof of Proposition 4. Estimates (44) of $\tilde{\boldsymbol{v}}_a$ are found first by rescaling (for a small enough)

$$\begin{aligned}\|\tilde{\boldsymbol{v}}_a\|^2_{L^2(\Omega)}=a^2\int_\Omega\Big|\,\boldsymbol{v}_\mathcal{B}[\boldsymbol{\nabla u}(\boldsymbol{z})]\Big(\frac{\boldsymbol{\xi}-\boldsymbol{z}}{a}\Big)\,\Big|^2\,\mathrm{d}V_\xi&=a^5\int_{(\Omega-\boldsymbol{z})/a}|\boldsymbol{v}_\mathcal{B}[\boldsymbol{\nabla u}(\boldsymbol{z})](\bar{\boldsymbol{\xi}})|^2\,\mathrm{d}\bar{V}_{\bar\xi}\\&\le a^5\int_{\mathbb{R}^3}|\boldsymbol{v}_\mathcal{B}[\boldsymbol{\nabla u}(\boldsymbol{z})](\bar{\boldsymbol{\xi}})|^2\,\mathrm{d}\bar{V}_{\bar\xi}=Ca^5\end{aligned}$$

(since the far-field behavior (38) implies that $\boldsymbol{v}_\mathcal{B}$ is square-integrable). Similarly,

$$\|\boldsymbol{\nabla}\tilde{\boldsymbol{v}}_a\|^2_{L^2(\Omega)}=a^2\int_\Omega\Big|\,\boldsymbol{\nabla}_\xi\boldsymbol{v}_\mathcal{B}[\boldsymbol{\nabla u}(\boldsymbol{z})]\Big(\frac{\boldsymbol{\xi}-\boldsymbol{z}}{a}\Big)\,\Big|^2\,\mathrm{d}V_\xi\le a^3\int_{\mathbb{R}^3}|\boldsymbol{\nabla}\boldsymbol{v}_\mathcal{B}[\boldsymbol{\nabla u}(\boldsymbol{z})](\bar{\boldsymbol{\xi}})|^2\,\mathrm{d}\bar{V}_{\bar\xi}=Ca^3$$

Furthermore, since $\boldsymbol{v}_\mathcal{B}=O(|\boldsymbol{x}|^{-2})$ and $\boldsymbol{\nabla}\boldsymbol{v}_\mathcal{B}=O(|\boldsymbol{x}|^{-3})$ at infinity by virtue of (38), one also deduces by rescaling that

$$\|\tilde{\boldsymbol{v}}_a\|_{L^\infty(\Omega\setminus D)}\le Ca^3\qquad\text{and}\quad\|\boldsymbol{\nabla}\tilde{\boldsymbol{v}}_a\|_{L^\infty(\Omega\setminus D)}\le Ca^3.\tag{B.1}$$

Attention is now directed towards the estimate (43) on $\boldsymbol{\delta}_a$. Combining (12) and a rescaled version of (15), the weak formulation satisfied by $\boldsymbol{\delta}_a$ is found as

$$\text{Find}\;\;\boldsymbol{\delta}_a\in W_0,\quad\langle\boldsymbol{\delta}_a,\boldsymbol{w}\rangle_\Omega^{\mathcal{C}_a}=-\langle\boldsymbol{u}-\boldsymbol{\varphi}[\boldsymbol{\nabla u}(\boldsymbol{z})],\boldsymbol{w}\rangle_{B_a}^{\Delta C}-G(\boldsymbol{w}),\quad\forall\boldsymbol{w}\in W_0$$

where $G(\boldsymbol{w})$ is defined as

$$G(\boldsymbol{w})=\langle\theta\tilde{\boldsymbol{v}}_a,\boldsymbol{w}\rangle_\Omega^{\mathcal{C}_a}+\langle\boldsymbol{\varphi}[\boldsymbol{\nabla u}(\boldsymbol{z})],\theta\boldsymbol{w}\rangle_{B_a}^{\Delta\mathcal{C}}$$

(having used that $\theta=0$ in $\mathbb{R}^3\setminus\Omega$ and $\theta=1$ in B_a). Taking $\boldsymbol{w}=\boldsymbol{\delta}_a$, one then has the following estimate:

$$C\|\boldsymbol{\varepsilon}[\boldsymbol{\delta}_a]\|^2_{L^2(\Omega)}\le|\langle\boldsymbol{\delta}_a,\boldsymbol{\delta}_a\rangle_\Omega^{\mathcal{C}_a}|\le|\langle\boldsymbol{u}-\boldsymbol{\varphi}[\boldsymbol{\nabla u}(\boldsymbol{z})],\boldsymbol{\delta}_a\rangle_{B_a}^{\Delta C}|+|G(\boldsymbol{\delta}_a)|.\tag{B.2}$$

The local smoothness assumption on $\boldsymbol{f}$ implies that $\boldsymbol{u}$ is C^2 at $\boldsymbol{z}$. Applying the mean value theorem, one then has

$$|\boldsymbol{\varepsilon}[\boldsymbol{u}](\boldsymbol{x})-\boldsymbol{\varepsilon}[\boldsymbol{u}](\boldsymbol{z})|\le Ca\;\text{ in }B_a,$$

so the first term in the right-hand side of (B.2) can be bounded as

$$|\,\langle \boldsymbol{u}-\boldsymbol{\varphi}[\boldsymbol{\nabla u}(\boldsymbol{z})],\boldsymbol{\delta}_a\rangle_{B_a}^{\Delta C}\,|\le Ca^{5/2}\|\boldsymbol{\varepsilon}[\boldsymbol{\delta}_a]\|_{L^2(\Omega)}.$$

Moreover, one has

$$G(\boldsymbol{\delta}_a)=\langle\theta\tilde{\boldsymbol{v}}_a,\boldsymbol{\delta}_a\rangle_{\Omega}^{\mathcal{C}_a}-\langle\tilde{\boldsymbol{v}}_a,\theta\boldsymbol{\delta}_a\rangle_{\Omega}^{\mathcal{C}_a}=\int_\Omega\Big\{\boldsymbol{\varepsilon}[\boldsymbol{\delta}_a]:\boldsymbol{\mathcal{C}}_a:(\tilde{\boldsymbol{v}}_a\otimes\boldsymbol{\nabla}\theta)^s-\boldsymbol{\varepsilon}[\tilde{\boldsymbol{v}}_a]:\boldsymbol{\mathcal{C}}_a:(\boldsymbol{\delta}_a\otimes\boldsymbol{\nabla}\theta)^s\Big\}\,\mathrm{d}V,$$

where the superscript 's' signifies the symmetric part. Hence, since $\boldsymbol{\nabla}\theta$ vanishes in a neighborhood D of B_a, by Korn's inequality and the estimates (B.1), it follows that

$$\begin{aligned}|G(\boldsymbol{\delta}_a)|&\le C\big[\,\|\tilde{\boldsymbol{v}}_a\|_{L^\infty(\Omega\setminus D)}+\|\boldsymbol{\varepsilon}[\tilde{\boldsymbol{v}}_a]\|_{L^\infty(\Omega\setminus D)}\,\big]\|\boldsymbol{\nabla}\theta\|_{L^2(\Omega\setminus D)}\|\boldsymbol{\varepsilon}[\boldsymbol{\delta}_a]\|_{L^2(\Omega)}\\&\le Ca^3\|\boldsymbol{\varepsilon}[\boldsymbol{\delta}_a]\|_{L^2(\Omega)}.\end{aligned}$$

Finally, from (B.2), the following global estimate holds:

$$\|\boldsymbol{\varepsilon}[\boldsymbol{\delta}_a]\|_{L^2(\Omega)}\le C(a^3+a^{5/2})\le Ca^{5/2},$$

completing the proof by Korn and Poincaré inequalities.

Appendix C. The equivalent inclusion approach. The concept of Eshelby tensor arises from considering a constant eigenstrain $\boldsymbol{E}^\star\in\mathbb{R}^{3,3}_{\mathrm{sym}}$ applied over an ellipsoidal part $\mathcal{B}$ of an unbounded elastic medium $\Omega=\mathbb{R}^3$ endowed with homogeneous elastic properties $\boldsymbol{\mathcal{C}}$ **[36]**. The displacement field $\boldsymbol{v}^\star_{\mathcal{B}}$ thus created is given explicitly by the representation formula

$$\boldsymbol{v}^\star_{\mathcal{B}}(\boldsymbol{x})=\langle\boldsymbol{\varphi}[\boldsymbol{E}^\star],\boldsymbol{G}_\infty(\cdot-\boldsymbol{x})\rangle_{\mathcal{B}}^{\mathcal{C}},\qquad\boldsymbol{x}\in\mathbb{R}^3\tag{C.1}$$

When $\mathcal{B}$ is an ellipsoid and $\boldsymbol{E}^\star\in\mathbb{R}^{3,3}_{\mathrm{sym}}$ is uniform, the above representation can be analytically evaluated, revealing that $\boldsymbol{v}^\star_{\mathcal{B}}$ depends linearly on $\boldsymbol{x}$ inside $\mathcal{B}$. The Eshelby tensor $\boldsymbol{\mathcal{S}}$ of B is then defined by setting

$$\boldsymbol{\varepsilon}[\boldsymbol{v}^\star_{\mathcal{B}}](\boldsymbol{x})=\boldsymbol{\mathcal{S}}:\boldsymbol{E}^\star\qquad(\boldsymbol{x}\in B).\tag{C.2}$$

Formula (56) for the components of $\boldsymbol{\mathcal{S}}$ stems from analytically evaluating (C.1) and interpreting the result according to definition (C.2).

Then, the equivalent inclusion method consists in finding an eigenstrain $\boldsymbol{E}^{\star\star}$ such that the solution $\boldsymbol{v}_{\mathcal{B}}$ of integral equation (35) has the form

$$\boldsymbol{v}_{\mathcal{B}}[\boldsymbol{E}]=\boldsymbol{\varphi}[\boldsymbol{\mathcal{S}}:\boldsymbol{E}^{\star\star}]\qquad\text{in }\mathcal{B}\tag{C.3}$$

Inserting the above ansatz in (35) and comparing with (C.1), the equivalent-inclusion analogy is found to be achieved by setting

$$\boldsymbol{E}^{\star\star}=-(\boldsymbol{\mathcal{C}}+\Delta\boldsymbol{\mathcal{C}}:\boldsymbol{\mathcal{S}})^{-1}:\Delta\boldsymbol{\mathcal{C}}:\boldsymbol{E}\tag{C.4}$$

Appendix D. Anisotropy index. The universal elastic anisotropy index, introduced in **[45]**, is defined as

$$A_{\mathrm{U}}=5\frac{\mu_{\mathrm{V}}}{\mu_{\mathrm{R}}}+\frac{\kappa_{\mathrm{V}}}{\kappa_{\mathrm{R}}}-6\ge0,\tag{D.1}$$

where $\boldsymbol{\mathcal{C}}_{\mathrm{V}}=3\kappa_{\mathrm{V}}\boldsymbol{\mathcal{J}}+2\mu_{\mathrm{V}}\boldsymbol{\mathcal{K}}$ and $\boldsymbol{\mathcal{C}}_{\mathrm{R}}=1/(3\kappa_{\mathrm{R}})\boldsymbol{\mathcal{J}}+1/(2\mu_{\mathrm{R}})\boldsymbol{\mathcal{K}}$ are the Voigt estimate of $\boldsymbol{\mathcal{C}}$ and the Reuss estimate of $\boldsymbol{\mathcal{C}}^{-1}$, respectively. Both estimates are defined from averaging over all possible spatial orientations, and are hence isotropic. They are given by $\boldsymbol{\mathcal{C}}_{\mathrm{V}}=\mathcal{H}(\boldsymbol{\mathcal{C}})$ and $\boldsymbol{\mathcal{C}}_{\mathrm{R}}=\mathcal{H}(\boldsymbol{\mathcal{C}}^{-1})$, where $\mathcal{H}$ is the Haar measure over the set of rotations of $\mathbb{R}^3$, defined by

$$\mathcal{H}(\boldsymbol{\mathcal{E}})=\frac{1}{8\pi^2}\int_0^{2\pi}\int_0^{2\pi}\int_0^{\pi}\boldsymbol{\mathcal{Q}}(\theta,\phi,\psi):\boldsymbol{\mathcal{E}}:\boldsymbol{\mathcal{Q}}^{\mathrm{T}}(\theta,\phi,\psi)\sin\theta\,\mathrm{d}\theta\,\mathrm{d}\phi\,\mathrm{d}\psi\tag{D.2}$$

(θ,ϕ,ψ denoting the Euler angles). In (D.2), the fourth-order rotation tensor $\boldsymbol{\mathcal{Q}}$ is defined (see **[48, 35]**) by $\boldsymbol{\mathcal{Q}}:=1/2(Q_{ik}Q_{j\ell}+Q_{i\ell}Q_{jk})\boldsymbol{e}_i\otimes\boldsymbol{e}_j\otimes\boldsymbol{e}_k\otimes\boldsymbol{e}_\ell$ in terms of the rotation matrix $\boldsymbol{Q}:=\boldsymbol{Q}_z(\psi)\boldsymbol{Q}_x(\theta)\boldsymbol{Q}_z(\phi)\in\mathbb{R}^{3,3}$,

where

$$\boldsymbol{Q}_z(\alpha) = \begin{pmatrix} \cos\alpha & -\sin\alpha & 0 \\ \sin\alpha & \cos\alpha & 0 \\ 0 & 0 & 1 \end{pmatrix}, \qquad \boldsymbol{Q}_x(\alpha) = \begin{pmatrix} 1 & 0 & 0 \\ 0 & \cos\alpha & -\sin\alpha \\ 0 & \sin\alpha & \cos\alpha \end{pmatrix}.$$

Acknowledgement. *The authors thank Prof. Grégoire Allaire (Centre de mathématiques appliquées, Ecole Polytechnique, Palaiseau, France) for many helpful discussions.*

REFERENCES

1. Eschenauer, H. A., Kobelev, V. V., Schumacher, A. Bubble method for topology and shape optimization of structures. *Structural Optimization*, **8**:42–51 (1994).

2. Schumacher, A. *Topologieoptimierung von Bauteilstrukturen unter Verwendung von Lochpositionierungskriterien*. Ph.D. thesis, Univ. of Siegen, Germany (1995).

3. Amstutz, S., Andrä, H. A new algorithm for topology optimization using a level-set method. *J. Comput. Phys.*, **216**:573–588 (2006).

4. Allaire, G., de Gournay, F., Jouve, F., Toader, A.-M. Structural optimization using topological and shape sensitivity via a level-set method. *Control and Cybernetics*, **34**:59–80 (2005).

5. Samet, B., Amstutz, S., Masmoudi, M. The topological asymptotic for the Helmholtz equation. *SIAM J. Control Optim.*, **42**:1523–1544 (2004).

6. Gallego, R., Rus, G. Identification of cracks and cavities using the topological sensitivity boundary integral equation. *Comp. Mech.*, **33**:154–163 (2004).

7. Feijóo, G. R. A new method in inverse scattering based on the topological derivative. *Inverse Prob.*, **20**:1819–1840 (2004).

8. Masmoudi, M., Pommier, J., Samet, B. The topological asymptotic expansion for the Maxwell equations and some applications. *Inverse Prob.*, **21**:547–564 (2005).

9. Bellis, C., Bonnet, M. A FEM-based topological sensitivity approach for fast qualitative identification of buried cavities from elastodynamic overdetermined boundary data. *Int. J. Solids Struct.*, **47**:1221–1242 (2010).

10. Kohn, R., McKenney, A. Numerical implementation of a variational method for electrical impedance tomography. *Inverse Prob.*, **6**:389–414 (1990).

11. Ladevèze, P., Leguillon, D. Error estimate procedure in the finite element method and applications. *SIAM J. Numer. Anal.*, **20**:485–509 (1983).

12. Deraemaeker, A., Ladevèze, P., Leconte, P. Reduced bases for model updating in structural dynamics based on constitutive relation error. *Comp. Meth. Appl. Mech. Eng.*, **191**:2427–2444 (2002).

13. Cedio-Fengya, D. J., Moskow, S., Vogelius, M. Identification of conductivity imperfections of small diameter by boundary measurements. Continuous dependence and computational reconstruction. *Inverse Prob.*, **14**:553–595 (1998).

14. Vogelius, M. S., Volkov, D. Asymptotic formulas for perturbations in the electromagnetic fields due to the presence of inhomogeneities of small diameter. *M2AN Math. Model. Num. Anal.*, **34**:723–748 (2000).

15. Maz'ya, V., Nazarov, S. A., Plamenevskii, B. A. *Asymptotic theory of elliptic boundary value problems under a singular perturbation of the domains (vols. 1 and 2)*. Birkhaüser (2000).

16. Il'in, A. M. *Matching of asymptotic expansions of solutions of boundary value problems*. American Mathematical Society (1992).

17. Ammari, H., Kang, H. *Polarization and moment tensors with applications to inverse problems and effective medium theory*. Applied Mathematical Sciences, Vol. 162. Springer-Verlag (2007).

18. Garreau, S., Guillaume, P., Masmoudi, M. The topological asymptotic for PDE systems: the elasticity case. *SIAM J. Contr. Opt.*, **39**:1756–1778 (2001).

19. Céa, J., Garreau, S., Guillaume, P., Masmoudi, M. The shape and topological optimization connection. *Comp. Meth. Appl. Mech. Eng.*, **188**:703–726 (2001).

20. Bonnet, M., Guzina, B. B. Sounding of finite solid bodies by way of topological derivative. *Int. J. Num. Meth. Eng.*, **61**:2344–2373 (2004).

21. Ben Abda, A., Hassine, M., Jaoua, M., Masmoudi, M. Topological sensitivity analysis for the location of small cavities in Stokes flow. *SIAM J. Contr. Opt.*, **48**:2871–2900 (2009).

22. Ammari, H., Kang, H., Nakamura, G., Tanuma, K. Complete asymptotic expansions of solutions of the system of elastostatics in the presence of an inclusion of small diameter and detection of an inclusion. *J. Elast.*, **67**:97–129 (2002).

23. Nazarov, S. A., Sokolowski, J., Specovius-Neugebauer, M. Polarization matrices in anisotropic heterogeneous elasticity. *Asympt. Anal.*, **68**:189–221 (2010).

24. Beretta, E., Bonnetier, E., Francini, E., Mazzucato, A. L. Small volume asymptotics for anisotropic elastic inclusions. *Inverse Prob. Imaging*, **6**:1–23 (2011).

25. Sokolowski, J., Zochowski, A. On the topological derivative in shape optimization. *SIAM J. Control Optim.*, **37**:1251–1272 (1999).

26. Giusti, S. M., Novotny, A. A., Padra, C. Topological sensitivity analysis of inclusion in two-dimensional linear elasticity. *Eng. Anal. Bound. Elem.*, **32**:926–935 (2008).

27. Silva, M., Matalon, M., Tortorelli, D. A. Higher order topological derivatives in elasticity. *Int. J. Solids Struct.*, **47**:3053–3066 (2010).

28. Guzina, B. B., Chikichev, I. From imaging to material identification: a generalized concept of topological sensitivity. *J. Mech. Phys. Solids*, **55**:245–279 (2007).

29. Guzina, B. B., Yuan, H. On the small-defect perturbation and sampling of heterogeneous solids. *Acta Mech.*, **205**:51–75 (2009).

30. Nazarov, S. A. Elasticity polarization tensor, surface enthalpy, and Eshelby theorem. *J. Math. Sci.*, **159**:133–167 (2009).

31. Leugering, G., Nazarov, S., Schury, F., Stingl, M. The Eshelby Theorem and Application to the Optimization of an Elastic Patch. *SIAM J. Appl. Math.*, **72**:512–534 (2012).

32. Ciarlet, P. G. *Mathematical elasticity. Volume 1 : Three-dimensional elasticity*. North Holland (1988).

33. Kupradze, V. D., ed. *Three-dimensional problems of the mathematical theory of elasticity and thermoelasticity*. North Holland (1979).

34. Eshelby, J. D. The determination of the elastic field of an ellipsoidal inclusion and related problems. *Proc. Roy. Soc. A*, **241**:376–396 (1957).

35. Mehrabadi, M. M., Cowin, S. C. Eigentensors of linear anisotropic elastic materials. *Quart. J. Mech. Appl. Math.*, **43**:14 (1990).

36. Mura, T. *Micromechanics of Defects in Solids*. Martinus Nijhoff (1987).

37. Allaire, G., Jouve, F., Van Goethem, N. Damage and fracture evolution in brittle materials by shape optimization methods. *J. Comput. Phys.*, **230**:5010–5044 (2011).

38. Bonnaillie-Noël, V., Dambrine, M., Tordeux, S., Vial, G. Interactions between moderately close inclusions for the Laplace equation. *Math. Models Meth. in Appl. Sc.*, **19**:1853–1882 (2009).

39. Samet, B. The topological asymptotic with respect to a singular boundary perturbation. *C.R. Acad. Sci. Paris, série I*, **336**:1033–1038 (2003).

40. Silva, M., Geubelle, P. H., Tortorelli, D. A. Energy release rate approximation for small surface-breaking cracks using the topological derivative. *J. Mech. Phys. Solids*, **59**:925–939 (2011).

41. Gavazzi, A., Lagoudas, D. On the numerical evaluation of Eshelby's tensor and its application to elastoplastic fibrous composites. *Comp. Mech.*, **7**:13–19 (1990).

42. Ting, T. C. T. *Anisotropic elasticity. Theory and applications*. Oxford (1996).

43. Ammari, H., Kang, H., Lee, H. A boundary integral method for computing elastic moment tensors for ellipses and ellipsoids. *J. Comput. Math.*, **25**:2–12 (2007).

44. Lebedev, V. I., Laikov, D. N. A quadrature formula for the sphere of the 131st algebraic order of accuracy. *Doklady Mathematics*, **59**(3):477–481 (1999).

45. Ranganathan, S. I., Ostoja-Starzewski, M. Universal elastic anisotropy index. *Phys. Rev. Lett.*, **101**:055504 (2008).

46. FreeFem++. A programming language and software for solving partial differential equations using the finite element method. Laboratoire Jacques-Louis Lions (Paris, France), http://www.freefem.org/ff++/index.htm (1985–2011).

47. Bonnet, M. Higher-order topological sensitivity for 2-D potential problems. Application to fast identification of inclusions. *Int. J. Solids Struct.*, **46**:2275–2292 (2009).

48. Cowin, S. C., Yang, G., Mehrabadi, M. Bounds on the effective anisotropic elastic constants. *J. Elast.*, **57**:1–24 (1999).

[a] POems (UMR 7231 CNRS-ENSTA-INRIA), ENSTA, Palaiseau, France, mbonnet@ensta.fr, [b] Centre de Mathématiques Appliquées (UMR 7641 CNRS-Ecole Polytechnique),, Ecole Polytechnique, Palaiseau, France, delgado@cmap.polytechnique.fr, [c] EADS-Innovation Works, Suresnes, France